2021

# INCORPORATING TEMPERATURE-DEPENDENT FISH BIOENERGETICS INTO A NARRAGANSETT BAY FOOD WEB MODEL

Margaret A. Heinichen
*University of Rhode Island*, mheinichen@gmail.com

# INCORPORATING TEMPERATURE-DEPENDENT FISH BIOENERGETICS INTO A NARRAGANSETT BAY FOOD WEB MODEL

BY

MARGARET A. HEINICHEN

A THESIS SUBMITTED IN PARTIAL FULFILLMENT OF THE

REQUIREMENTS FOR THE DEGREE OF

MASTER OF SCIENCE

IN

OCEANOGRAPHY

UNIVERSITY OF RHODE ISLAND

2021

MASTER OF SCIENCE THESIS

OF

MARGARET A. HEINICHEN

APPROVED:

Thesis Committee:

Major Professor Jeremy Collie

Austin Humphries

Coleen Suckling

M. Conor McManus

Brenton DeBoef
DEAN OF THE GRADUATE SCHOOL

UNIVERSITY OF RHODE ISLAND
2021

**ABSTRACT**

Food web models capture shifting species interactions, making them useful tools for exploring community responses to perturbations. The inclusion of environmental drivers, such as temperature, can improve model predictions as energy demands of an organism can be temperature-specific. While Ecopath with Ecosim (EwE) and the recent R implementation of this software, Rpath, have included some thermal responses in past work, models have yet to include temperature-dependent energetic demands and metabolic costs. Our work demonstrates the inclusion of temperature-dependent bioenergetics into an Rpath food web model using the case study of a warming estuary: Narragansett Bay (RI, U.S.). Thermal response parameters from literature were used to construct Kitchell curves describing temperature-dependent consumption and modified Arrhenius curves describing temperature-dependent respiration. Surface water temperature time series from 1994 to 2054 for high and low warming scenarios were created from observed temperatures and projections from the Coupled Model Intercomparison Project (CMIP6) multi-model ensemble. The integration of temperature-dependent fish bioenergetics resulted in lower projected biomasses compared to the base version of the model without environmental forcing, reflecting the impact of increased energetic demands. The differences in the model-predicted biomasses highlight the importance of accounting for thermal effects on marine species in ecosystem models, which will become increasingly important as ocean temperatures continue to rise in Narragansett Bay and worldwide.

**ACKNOWLEDGMENTS**

I would like to thank my advisor, Jeremy Collie, who has helped me grow as a researcher during my time at GSO. This work would not have been possible without Annie Innes-Gold whose wonderful attitude helped me succeed. She was instrumental in the creation of the base model, and she will forever be my best and favorite Ecopath partner. I would also like to thank Joe Langan and Nina Santos, as well as all other former Collie lab students for their generous support over the last two and a half years. Thank you to Austin Humphries and Conor McManus for their continued assistance when creating my bioenergetic model. I am extremely grateful to RI C-AIM for financial support, and a particular shout out to BJ Carangia and Shaun Kirby for answering my many questions. Finally, thank you to my wonderful parents, family, friends, and my fiancé, Mike, for their continued love and support through this process.

## PREFACE

The following thesis has been submitted in manuscript format following the formatting guidelines of the journal *Ecological Modelling*.

**TABLE OF CONTENTS**

## LIST OF TABLES

TABLE PAGE

**LIST OF FIGURES**

FIGURE PAGE

**CHAPTER 1**

# Incorporating temperature-dependent fish bioenergetics into a Narragansett Bay food web model.

Margaret Heinichen[*a], M. Conor McManus[b], Sean Lucey[c], Kerim Aydin[d], Austin Humphries[e,a], Anne Innes-Gold[e], Jeremy Collie[a]

Manuscript in preparation for submission to the journal *Ecological Modelling.*

[a]Graduate School of Oceanography, University of Rhode Island, 215 South Ferry Rd, Narragansett, RI 02882, United States

[b]Rhode Island Department of Environmental Management, Division of Marine Fisheries, 3 Ft. Wetherill Rd., Jamestown, RI 02835, United States

[c]NOAA, National Marine Fisheries Service, Northeast Fisheries Science Center, 166 Water Street, Woods Hole, MA 02543, United States

[d]NOAA, National Marine Fisheries Service, Alaska Fisheries Science Center, 7600 Sand Point Way NE, Seattle, WA 98115, United States

[e]Department of Fisheries, Animal and Veterinary Sciences, University of Rhode Island, Kingston, Rhode Island

* Corresponding Author.
*Email Address*: mheinichen@uri.edu
Present address: 235 Coastal Institute Building, 215 South Ferry Rd, Narragansett, RI 02882

**Keywords**
Food web model, fish bioenergetics, Rpath, estuary, climate change, thermal responses

**Abstract**

Food web models capture shifting species interactions, making them useful tools for exploring community responses to perturbations. The inclusion of environmental drivers, such as temperature, can improve model predictions as energy demands of an organism can be temperature-specific. While Ecopath with Ecosim (EwE) and the recent R implementation of this software, Rpath, have included some thermal responses in past work, models have yet to include temperature-dependent energetic demands and metabolic costs. Our work demonstrates the inclusion of temperature-dependent bioenergetics into an Rpath food web model using the case study of a warming estuary: Narragansett Bay (RI, U.S.). Thermal response parameters from literature were used to construct Kitchell curves describing temperature-dependent consumption and modified Arrhenius curves describing temperature-dependent respiration. Surface water temperature time series from 1994 to 2054 for high and low warming scenarios were created from observed temperatures and projections from the Coupled Model Intercomparison Project (CMIP6) multi-model ensemble. The integration of temperature-dependent fish bioenergetics resulted in lower projected biomasses compared to the base version of the model without environmental forcing, reflecting the impact of increased energetic demands. The differences in the model-predicted biomasses highlight the importance of accounting for thermal effects on marine species in ecosystem models, which will become increasingly important as ocean temperatures continue to rise in Narragansett Bay and worldwide.

## 1. **Introduction**

Climate change represents a major continuous perturbation to the Northeast U.S. Continental Shelf ecosystem, affecting species distribution, migration phenology, and physiological processes (Chabot et al., 2016; Kleisner et al., 2017; Langan et al., 2021; Pershing et al., 2015). Rises in sea temperature have been acutely observed in Narragansett Bay, Rhode Island (U.S.), where surface water temperatures have risen approximately 1.5°C since 1950 (Fulweiler et al., 2015). Climate-driven models can help elucidate how these changes in temperature are affecting ecosystem dynamics (Brander, 2015). Food web models, such as those created using the Ecopath with Ecosim (EwE) software, are becoming increasingly popular to study how ecosystems respond to changes in fisheries harvest, species interactions, and external drivers (Buchheister et al., 2017; Colléter et al., 2015; Villasante et al., 2016). While some studies have included environmental components (Bentley et al., 2017; Corrales et al., 2017; Serpetti et al., 2017), there are thermal influences on marine populations, such as direct impacts on species bioenergetic demands, that have not yet been incorporated into EwE models.

As ectotherms, fish rely on the environment to regulate their body temperature, with ambient temperatures ultimately influencing physiological rates (Jobling, 1994). These individual-level metabolic processes and life history rates of organisms can scale up to impact ecosystems (Humphries and McCann 2014; Chabot et al. 2016). Consequently, bioenergetics and physiological responses are often used as the basis for mechanistically-driven models (Jørgensen et al. 2016). The basics of temperature-dependent bioenergetics have been recognized for decades (Brett, 1971; Jobling,

1994), and while species-specific rates are often unknown, it is nonetheless important to begin incorporating bioenergetic relationships into multispecies ecosystem models for increased realism of how species dynamics are affected by warming waters. Understanding community responses to climate change, rather than examining single-species responses in isolation, will provide more insight as to how environmental stressors will affect marine ecosystems (Nagelkerken and Munday 2016).

As temperatures increase from the cooler portion of a species' thermal tolerance, it can become more energetically expensive for ectotherms to maintain base metabolic demands (Chabot et al., 2016; Jobling, 1994). The thermal response of metabolism is frequently described with an Arrhenius equation (Eq. (1)) if thermodynamic relationships are considered the dominant drivers (Brown et al., 2004; Gillooly et al., 2001; Schulte, 2015). The Arrhenius equation, often used in fitting laboratory data or in models incorporating metabolic ecology (Blanchard et al., 2012; Clarke and Johnston, 1999; Dahlke et al., 2020; Neubauer and Andersen, 2019), calculates the rate of reaction ($k$) as a function of a constant ($A$), the activation energy ($E_a$), the universal gas constant ($R$), and the temperature ($T$) in degrees kelvin.

$$k = Ae^{-E_a/RT} \quad (1)$$

Temperature-dependent energetic costs can modify species interactions, primarily through the adjustment of consumption rates as predators alter their intake to maintain their energy balance (Johansen et al., 2015). In relation to temperature, consumption increases as waters warm, reaches a maximum at some optimum temperature, and then ingestion sharply decreases as the maximum tolerated temperature is approached (Fogarty and Collie, 2020; Jobling, 1994). Increasing

consumption with increasing temperatures has been documented for a variety of fishes including bluefish (*Pomatomus saltatrix*), brook trout (*Salvelinus fontinalis*), and anemonefish (*Amphiprion melanopus*) (Buckel et al., 1995; Nowicki et al., 2012; Olla et al., 1985; Ries and Perry, 1995). Increased metabolic demand in warmer waters likely accounts for the increasing portion of the curve, while stress responses and behavioral shifts are thought to drive the reduced consumption rates frequently seen near species' thermal maxima (Brett, 1971; Jobling, 1997; Johansen et al., 2014; Nowicki et al., 2012). The exact shape can vary due to the many factors affecting consumption, such as locomotion, hormone regulators, detection, and successful prey capture, but numerous experimental studies have documented this general thermal response (Jobling, 1997; Volkoff and Rønnestad, 2020).

Higher energetic demands can adversely affect production, or the surplus energy available for optional processes such as growth and reproduction (Jobling, 1994; Neubauer and Andersen, 2019). Temperature can adjust the efficiency with which organisms transform food energy into growth (Lemoine and Burkepile, 2012). Given that the foundational bioenergetic relationships apply to many marine species operating in their preferred thermal range (Deslauriers et al., 2017; Sibly et al., 2012), the integration of temperature-dependent bioenergetics in ecosystem models can provide more realistic predictions of how climate change will impact ecosystem production (McKenzie et al., 2016).

The EwE software has been used to model over 400 marine and aquatic ecosystems (Colléter et al., 2015). Ecopath creates static, mass-balance food web models that give a snapshot of the energy flow of an ecosystem (Polovina, 1984).

Ecopath is governed by master equations for consumption and production and requires data inputs of biomass (*B*), production to biomass ratio (*P/B*), consumption to biomass ratio (*Q/B*), a diet matrix, and fishing information (Christensen and Pauly, 1992). Ecosim expands this snapshot to create time-dynamic projections of biomass (Coll et al., 2009). Predation is modeled with foraging arena theory in which prey are, at times, vulnerable to predation and invulnerable at others (Ahrens et al., 2012; Walters and Christensen, 2007). The vulnerabilities, or the parameters specifying the rate of exchange between vulnerable and invulnerable states, are estimated with a fitting procedure to minimize the sum of squares between projected and observed biomasses (Heymans et al., 2016). External forcing functions of changing inputs, such as primary production or fishing effort, can also be used to drive the dynamic models into the future (Christensen and Walters, 2004).

Recent enhancements of the EwE software allow for greater use of environmental forcing functions, with some researchers incorporating a thermal modifier of species consumption (Bentley et al., 2017; Corrales et al., 2018; Serpetti et al., 2017) or temperature-dependent recruitment (Bentley et al., 2020). The models with temperature-dependent consumption used temperature of occurrence to estimate thermal preference, and modified consumption to restrict foraging capacity for each species or functional group. However, no EwE model has so far incorporated the other major energetic impact of temperature: changing energy demands and metabolic costs. One of the master equations of Ecopath specifies that consumption in units of biomass consumed is the sum of production, respiration, and unassimilated food ($C = P + R + U$ ; Christensen et al. 2005). EwE aggregates metabolic costs into the respiration term

which represents the biomass lost to the ecosystem (i.e. energy consumed and assimilated by a group but is not transformed into production). Thermal adjustments to the respiration term are not in the current EwE software capacity. However, EwE-type food web models can now be created and investigated in the flexible R software using the 'Rpath' package (Lucey et al., 2020). The Rpath package creates an opportunity for further exploration of the ecosystem responds to shifting environmental conditions and the inclusion of temperature-dependent bioenergetics.

The goal of this study is to demonstrate how temperature-dependent bioenergetics can be incorporated in a food web model using Rpath, the flexible R implementation of the Ecopath with Ecosim modeling framework. We apply this method to better understand climate change impacts using a rapidly warming Narragansett Bay as a case study. We hope to expand the functionality of Rpath and illustrate the scales at which temperature-dependent consumption and respiration can amplify to alter food web model biomass outputs.

## 2. Methods

### 2.1 Base model

Our work built upon a preexisting EwE model of Narragansett Bay (Rhode Island, U.S.). Innes-Gold et al. (2020) described a yearly and spatially averaged, functional group based food web model of Narragansett Bay. The starting Ecopath model was built using averaged 1994-1998 data. The dynamic Ecosim model was fitted to observed biomass data from 1994 to 2018. The model has 15 functional groups (Supplemental Table A1.1), with 28 species of commercial, recreational, or ecological importance assembled into the upper trophic level groups based on diet

similarity. The EwE model did not include any explicit environmental forcing. Further information on the model can be found in Innes-Gold et al. (2020).

The Narragansett Bay model was reformatted for compatibility with the R package 'Rpath' described in Lucey et al. (2020) using R version 3.6.0 (R Core Team, 2019). The Ecopath model became a static Rpath model, and the dynamic Ecosim model became an Rsim model. The Rsim model was projected from 1994 to 2054, and the forcing functions of the original Ecosim model (i.e. phytoplankton biomass, cultured shellfish biomass, and fishing mortality) were held constant from 2019 to 2054 at the present-day levels (average of the 2014-2018 values). Further details on the Rpath input of the model can be found in Supplement A.1. The Rsim output projected through 2054 without temperature forcing was considered the 'base' version of our model.

For the model versions with temperature-dependent bioenergetics, thermal responses were only included for the fish functional groups (planktivorous fish, benthivorous fish, and piscivorous fish). There is greater availability of bioenergetic data for the modeled fish species compared to the invertebrate species, and the thermal responses of other taxa may be best represented with different functional forms than those used for fish. Thermal response parameters were collected for each of the 19 species (Supplemental Table A1.2) that compose the fish functional groups.

### 2.2 Temperature

Surface water temperatures were taken from the University of Rhode Island Graduate School of Oceanography (URI GSO) weekly fish trawl (Collie et al., 2008). Before 2007, temperature was measured with a thermometer from water samples

collected at the surface and bottom; since 2007 a YSI® (Model 6920 V2) multi-parameter water quality sonde has been used (URI GSO, 2021). Occasional missing temperatures were estimated based on imputations calculated from generalized additive models (GAMs) as described in Langan et al. (2021). Only the temperatures recorded from the Fox Island station were used in our study, as this mid-Bay station was thought to be a more representative average of the temperatures experienced in the Bay than the lower Bay Whale Rock station. Surface temperature was examined instead of bottom temperature because both benthic and pelagic fish species were assessed, and fewer correlations were needed to predict surface water temperature in the projections through 2054. Since the food web model was yearly averaged, annual average temperatures from 1994 to 2018 were calculated as the average of each monthly temperature to account for unequal sampling effort in some months.

Temperature projections for Narragansett Bay were constructed to discern how the Narragansett Bay ecosystem may change in the future when accounting for temperature-dependent bioenergetics. First, grid cells' data which included Narragansett Bay from six models of the Coupled Model Intercomparison Project 6$^{th}$ phase (CMIP6) multi-model ensemble were accessed. The two warming scenarios tested were a low warming scenario from Shared Socioeconomic Pathway 1-2.6 (SSP1-2.6) and a 'business as usual' high warming scenario with SSP5-8.5 (O'Neill et al. 2016, Eyring et al. 2016; Supplemental Table A2.1). The air temperature projections from the six CMIP6 models were delta corrected and linearly transformed to project yearly averaged surface water temperatures following the methods described in Bell et al. (2018). To bias correct the projections, delta corrections were applied

between the CMIP6 modeled air temperature and observed air temperature as well as observed water temperature and projected water temperature. Air temperature data from the National Oceanic and Atmospheric Administration (NOAA) National Centers for Environmental Information for the TF Green Airport, Providence, RI station were used to relate observed air temperature to observed surface water temperatures (www.ncdc.noaa.gov; Supplemental Table A2.2). Temperatures were projected through 2054 based on data availability. This projection timeframe is long enough to see distinct changes in the average Bay temperature, while being short enough to provide reasonable projection results, since physiological responses can adjust on shorter timescales through acclimation (i.e. physiological adjustment to new, sustained conditions) and adaptation, and on longer timescales (i.e. yearly to decadal) through range shift, ecological feedbacks, and evolution (Peck, 2011; Sibly et al., 2012). The final time series for the high and low warming scenarios were created by averaging the output of each of the six delta corrected surface temperature projections for each year after 2018.

### 2.3 Temperature-dependent consumption

The food consumption thermal response for each of the three fish functional groups was described using the Kitchell equation (Hansen et al., 1997; Kitchell et al., 1977), which is routinely used to characterize temperature-dependent consumption in bioenergetic models (Hansson et al., 1996; Harvey, 2009; Luo and Brandt, 1993). The Kitchell equation, shown in Eq. (2), uses straightforward input parameters of the thermal maximum ($T_{max}$; the temperature above which consumption is zero), temperature of optimum consumption ($T_{optC}$), and the $Q_{10}$ of consumption (referring to

the rate of change for a process as the temperature increases 10°C; Hansen et al. 1997, Fogarty & Collie 2020) to estimate the proportion of maximum consumption that occurs at a given temperature ($r_c$).

$$r_c = \left[\frac{T_{max} - T}{T_{max} - T_{optC}}\right]^X * e^{\left[X*\left(1-\frac{T_{max}-T}{T_{max}-T_{optC}}\right)\right]} \quad (2)$$

$$where\ X = \left\{\frac{\left[\ln(Q_{10})*(T_{max}-T_{optC})\right]^2}{400}\right\} * \left\{1 + \left[1 + \left(\frac{40}{\ln(Q_{10})*(T_{max}-T_{optC}+2)}\right)^{0.5}\right]^2\right\}$$

The three thermal parameters ($T_{max}$, $T_{optC}$, $Q_{10}$) for each fish species were derived from the literature, and a hierarchy of data sources was used to choose the value for each parameter (Supplement A.3). The original Innes-Gold et al. (2020) model was parameterized for adult fish; for compatibility, literature values for adults were chosen over those for younger life stages. Additionally, experimental studies were chosen over values reported from other models. For each species, $T_{max}$ was chosen as the highest value from temperature of occurrence data in Narragansett Bay, stock-wide temperature of occurrence from the website Aquamaps (Kaschner et al., 2019; www.aquamaps.org), or studies focusing on thermal tolerance. For some species, limited information required the assumption of relationships between $T_{optC}$, $T_{max}$, and a described temperature of maximum growth in order to estimate $T_{optC}$ in the absence of published consumption data. The $Q_{10}$ is assumed to be 2.3 when no other estimate is available (Hansen et al., 1997). Effort was made to choose values from studies that were the most representative of the fish in Narragansett Bay, but, particularly in the case of $T_{optC}$, we were limited by the information available in the literature.

Consumption thermal response by functional group began with the species-specific Kitchell input parameters. A biomass weighted average of species from 1994-1998 (Supplemental Table A3.4) yielded the parameters by functional group, which were then inputted to the Kitchell equation. The weighting of the consumption curve, therefore, was weighted the same as the other original Ecopath parameters (Innes Gold et al., 2020). Modelling bioenergetic responses on a functional group level smoothed intra- and inter-species variability in thermal response. The challenge of determining an appropriate level of aggregation when integrating physiological responses in models has been recognized by others (Cooke et al., 2014), but our method was the most consistent with the parameterization of the original EwE model.

We ran a sensitivity test to examine the effect of input community composition on the consumption thermal response curves. Three Kitchell curves per functional group, weighted by different species biomasses, were used to create consumption modifier time series; 1) the 1994-1998 averaged biomasses as described earlier in the methods, 2) the single year's observed biomass from the time series data that resulted in the strongest warm-skewed curve, and 3) biomasses including more southern, warm-water species to represent a future curve as new species enter the Bay. Further information on the creation of the curves with southern species can be found in Supplement Table A4.1.

The thermal response curves were adjusted to account for the temperature at which the Ecopath baseline was established. The standard Kitchell curve ranges between 0 and 1. In the EwE framework, Ecosim models build off the Ecopath starting conditions. In our case, the Ecopath model represented the average Bay state in 1994-

1998. The scaling of the curve grounded the thermal response in the starting conditions of the initial Ecopath model. We scaled the Kitchell curve so that the thermal modifier was 1.0 at the average 1994-1998 temperature of the Bay ($T_{B94}$; Eq. (3)). The scaled Kitchell curve, referred to as the relative consumption curve (*RelC*), had a maximum consumption modifier greater than one at $T_{optC}$.

$$RelC = Kitchell_{orig} / \left( Kitchell_{orig}|_{T_{B94}} \right) \quad (3)$$

The base model with temperature-dependent consumption will be referred to as the 'consumption' version of the model. Temperature-dependent consumption was forced differently than previous EwE models because the forcing functions between Ecosim and Rsim differ. In this study, the consumption modifiers, as calculated from the relative consumption curve and temperature time series, were applied with the 'ForcedSearch' feature (formerly called ForcedPred). This forcing option modifies the effective predator biomass which is then inputted into the main consumption calculations (Lucey et al. 2020 equations 19 & 20). The calculations of ForcedSearch function apply the thermal response before the full consumption calculations, so that the foraging arena and interspecies interactions mediate the temperature effect on physiological processes, as has been suggested by others (Neubauer and Andersen, 2019). A time series of consumption modifiers by year then forced the temperature-dependent model versions using the 'adjust.forcing' function on the ForcedSearch parameter.

### 2.4 Temperature-dependent respiration

The second bioenergetic response built into Rpath was temperature-dependent respiration. Respiration was treated similarly to standard metabolism, though

respiration includes other energetic costs including standard dynamic action (SDA), the metabolic cost to digest food, or activity costs. Our framing of metabolism as the amount of energy used to maintain function was more directly applicable to the EwE mass-balance setup and respiration term than other metrics such as aerobic scope. The original Innes-Gold et al. (2020) EwE model was a parsimonious model of the ecosystem in which species age and size were generally not included. Therefore, our functional form for temperature-dependent respiration was simplified because it did not include a body mass effect on respiration (Sibly et al., 2012). This simplification was appropriate since the fish groups in the base model were not multi-stanza (i.e. subdivided into size or age groups), and size structure of the population was not modelled.

Though the literature often describes respiration as an exponential increase of base metabolic energy demand with temperature, many experimental studies only reported two- to four-fold increases in standard or resting metabolism (Bernreuther et al., 2013; Dalla Via et al., 1998; Johansen and Jones, 2011; Sandersfeld et al., 2017; Schwieterman et al., 2019; Slesinger et al., 2019; Stewart and Binkowski, 1986). Studies investigating the relationship between temperature and metabolic costs have included SDA or locomotion, but similar ranges of metabolic increases were reported (Fu et al., 2009; Hartman and Brandt, 1995). Therefore, we thought that including resting metabolism, SDA, and activity should only increase energetic losses to metabolism by a factor of eight to ten-fold over biologically relevant temperatures.

The modified Arrhenius equation reported in Blanchard et al. (2012) calculated with their reported parameters was used as the functional form for the thermal

response of fish respiration in relationship to temperature (Eq. (4)). The thermal modifier (τ), ranging from zero to ten, is a function of the temperature in degrees kelvin, the Boltzmann constant (k; $8.62 \times 10^{-5}$ eV $K^{-1}$), the activation energy (0.63 eV; similar to values in other studies such as Gillooly et al. 2001, Brown et al. 2004), and a constant (c1=25.55).

$$\tau = e^{c1-(E/kT)} \quad (4)$$

The modified Arrhenius equation is the best fit for constraining the metabolic modifier to the range of increases seen in literature for these and similar species. However, there are no species-specific parameters. Given that any species-specific thermal responses would be clouded in the base model's aggregation to functional groups, we considered the Blanchard et al. (2012) equation to adequately represent a generalized (i.e. non-species specific) fish metabolic thermal response. The respiration thermal response was scaled using similar methods to the consumption response scaling, so that a modifier of τ=1 on the relative respiration curve (*RelR*; i.e. scaled Blanchard curve) was associated with $T_{B94}$ (Eq. (5)).

$$RelR = Blanchard_{orig} / \left( Blanchard_{orig}|_{T_{B94}} \right) \quad (5)$$

Production rate (*P/B*) is static, and respiration is solved for in the default programming of Ecopath. Rsim uses a parameter, ActiveRespFrac, to represent the fraction of energy devoted to respiration, which is calculated from the production to consumption ratio and unassimilated food (Aydin et al., 2016). The ActiveRespFrac parameter is carried through the dynamic Rsim simulations. Unassimilated food is assumed to be independent of temperature.

The first step in creating the time series used to force temperature-dependent respiration was to multiply the relative consumption curves by the Ecopath total consumption, equal to Ecopath *Q/B* multiplied by biomass, to make a curve of total consumption by temperature (Eq. (6)).

$$TotalCons_T = RelC * Q/B_{Ecopath} * Biomass_{Ecopath} \quad (6)$$

The total consumption at $T_{B94}$ for each of the functional groups was multiplied by the base ActiveRespFrac to get the total respiration at $T_{B94}$. The relative respiration curve was multiplied by the ratio of the total respiration at $T_{B94}$ to the relative respiration modifier value at that temperature which produced a total respiration by temperature curve (Eq. (7)).

$$TotalResp_T = RelR * \left(TotalCons_T|_{T_{B94}} * ActiveRespFrac_{Base}\right) / RelR|_{T_{B94}} \quad (7)$$

Dividing the total respiration by total consumption gave ActiveRespFrac by temperature (Eq. (8)).

$$ActiveRespFrac_T = TotalResp_T / TotalCons_T \quad (8)$$

In another sensitivity test, we scaled the consumption and respiration curves to the temperatures that informed the original parameters estimated in the Ecopath model to examine the sensitivity of the curves to the implicit thermal parameterization of the Ecopath model and different scaling temperatures. In this sensitivity test, the Kitchell curves were scaled to the temperature informing the Ecopath *Q/B* parameters ($T_{QB}$) instead of the temperature of the Bay ($T_{B94}$). The Blanchard curve was scaled by the temperature of fishing mortality ($T_F$; $T_F = T_{B94}$ as the fisheries catches used to calculate fishing mortality were taken from the Bay) and the temperature of natural

mortality ($T_M$; mean($T_Z$, $T_M$)=$T_{PB}$). The average temperatures of the Ecopath parameters for the fish functional groups can be found in Supplemental Table A4.2.

The bioen branch of Rpath development introduces the ForcedActresp function (github.com/NOAA-EDAB/Rpath). This function modifies the total energetic losses to respiration (ActiveRespLoss). The respiration modifier at each year ($t$) was calculated so that ActiveRespFrac for each year was what would be expected from the temperature time series and the ActiveRespFrac by temperature curves (Eq. (9)).

$$ForcedActresp_t = ActiveRespFrac_{T,t} \,/\, ActiveRespFrac_{Base} \quad (9)$$

**2.5 Comparison of model versions**

Three model versions with two warming scenarios were compared (Table 1). The static starting conditions of all model versions was the Rpath translation of the 1994-1998 average Ecopath model of Innes-Gold et al. (2020). The Rsim translation of the Innes-Gold et al. (2020) Ecosim model of Narragansett Bay was the base version. Temperature-dependent consumption only was included in the consumption version of the model, and both temperature-dependent consumption and respiration were included in the respiration version of the model (Figure 1). The consumption and respiration versions were forced with observed temperatures from 1994-2018, and two warming scenarios, high and low, were used to project the consumption and respiration model versions from 2019 to 2054. Versions of the model were compared in terms of fit (i.e. sum of squares between Rpath modeled absolute biomass and observed biomass), realism of bioenergetic responses to temperature, and future projected biomasses.

The third and final sensitivity test performed examined the influence of the vulnerability parameter, given we expected the vulnerability parameters to have strong impacts on resulting biomasses. The Qlink values (i.e. measure of energy transferred between a predator and prey) for which the fish were predators and output biomasses in the respiration model version with the high warming scenario were compared for three sets of vulnerabilities: the original values used in the Innes-Gold et al. (2020) model, a 20% change in vulnerabilities whereby each vulnerability was adjusted 20% closer to the default of 2, and the EwE default 2.0 for all vulnerabilities.

## 3. Results

### 3.1 Temperature

There was strong interannual variability in the observed, averaged surface temperatures from 1994-2018; however, there was no apparent warming trend (Figure 2). The $T_{B94}$ temperature was 11.7°C. The historical temperatures of the CMIP6 models were generally comparable to observed temperatures. Each CMIP6 model had similar variability to the observed time series which was dampened when averaging the climate models together. However, this forward projection with lower variability still captured warming trends presented by the multi-model ensemble. The high warming scenario, SSP5-8.5, provided an overall increase of nearly 3°C between the start of the time series and 2050. The low warming SSP1-2.6 yielded an average increase of approximately 2°C by 2050. The greatest difference between the high and low warming scenario projections was 1.1°C in 2045.

### 3.2 Consumption response curves

The thermal response curves for consumption generally reflected the shape as suggested by theory (Figure 3A). The curves varied between functional groups with piscivorous fish having the steepest increase in consumption below $T_{optC}$, while benthivorous fish had the steepest decrease near their thermal maximum. The input species for these curves generally had broad thermal tolerances, and the average temperatures experienced in Narragansett Bay were on the lower end of their tolerance ranges (Supplemental Figure B2.1).

The thermal modifiers of all functional groups increased over 1.0 early in the time series, though within each functional group the modifier only varied by 0.2-0.5 (Figure 3B). The ending consumption modifier was larger in the high warming scenario for all fish groups, and piscivorous fish had the largest consumption modifier overall (maximum=1.38). The community composition sensitivity test resulted in relative consumption curves with different thermal maxima, but the consumption modifier time series were similar as the curves overlap at the colder average temperatures of the Bay (Supplemental Figure B2.2). The curves created from a single year's observed biomasses were more extreme than the curves created with moderate biomasses of new southern species.

### 3.3 Respiration response curves

The original Blanchard curve had a thermal modifier of 1.0 at 13°C, thus the Blanchard curve and the relative respiration curve scaled to $T_{B94}$ were similar (Figure 4A). The three ActiveRespFrac curves by temperature varied by functional group due to the interplay between the respiration and consumption curves (Figure 4B). The

planktivorous fish ActiveRespFrac curve was relatively flat before steeply increasing near maximum temperatures. The benthivorous fish curve showed an increasing trend as waters warm (from 0.54 to 0.74 from 0°C to 20°C). The piscivorous fish ActiveRespFrac decreased to a minimum of energy allocated to metabolism (41%) occurring at 18.4°C before sharply increasing. The temperature-dependent production, shown by the balance of temperature-dependent consumption and respiration, varied in shape by functional group (Supplemental Figures B3.1A-B3.1C). Piscivorous fish had the most defined temperature-production curve, in which the temperature of maximum potential production was slightly cooler than the temperature of maximum consumption. The planktivorous fish production-temperature curve was less pronounced, and there was a very minor curve in the energy available for production for benthivorous fish.

ActiveRespFrac forcing varied between the high and low projected warming scenarios (Figure 4C). In the base version of the model, piscivorous fish had the lowest ActiveRespFrac (0.48), followed by planktivorous fish (0.53), and benthivorous fish had the highest (0.61). Both planktivorous fish and benthivorous fish ActiveRespFrac only varied by 0.03 throughout the time series. Both groups had higher ending metabolic demands compared to the starting conditions of the Rpath model. Unlike the other two functional groups, piscivorous fish ActiveRespFrac declined during the 60-year projection, as the temperatures experienced by the Bay during this period were still on the decreasing portion of their ActiveRespFrac curve.

Under the second sensitivity test, the scaling temperature chosen for the relative consumption and respiration curves varied by functional group. The $T_{QB}$ for

piscivorous fish was much higher than $T_{B94}$, which was reflected in the relative consumption curve for that functional group (Supplemental Figure B3.2A). The consumption for piscivorous and benthivorous fish remained below the respective Ecopath starting points for the entirety of the time series (Supplemental Figure B3.2B). For respiration, the $T_{PB}$ was similar to $T_{B94}$, so that the ActiveRespFrac by temperature curves differed slightly (Supplemental Figures B3.3A-B3.3B). The ActiveRespFrac time series had similar increasing or decreasing patterns by functional group but were scaled differently relative to the initial ActiveRespFrac (Supplemental Figure B3.3C). In this test, piscivorous fish had respiration costs higher than their baseline in all years.

### 3.4 Comparison of model versions

The inclusion of temperature-dependent fish bioenergetics impacted the modelled biomasses (Figure 5). For planktivorous and benthivorous fish, the consumption model versions yielded higher ending biomasses than the base model, and the respiration model versions yielded lower biomasses in warming water (Figure 6). Planktivorous fish and benthivorous fish biomasses were 14.55 g/m$^2$ and 9.93 g/m$^2$ in the high warming respiration version compared to 17.03 g/m$^2$ and 12.46 g/m$^2$ in the high warming consumption version. Piscivorous fish biomass was highest in the high warming respiration model version (9.25 g/m$^2$) due to their respiration costs decreasing as water temperature increased from its current state.

Piscivorous fish had the greatest percent difference in the 2054 biomass estimates between of the five tested model versions and scenarios (28% between the high warming respiration version and the base version of the model). The other fish

groups varied by 14.6% (planktivorous fish) and 20.3% (benthivorous fish). The carnivorous benthos group differed by 20.4% at most, with biomasses approximately 2 $g/m^2$ lower in the consumption versions than the base version. Although the absolute biomasses were small, squid groups differed by 18-27% between model versions, with the base model version predicting the highest biomasses. These groups had stronger connections to the adjusted fish groups than the other mid and lower trophic level groups which had biomass vary between model versions by 1-6%.

The model version with the best fit (i.e. lowest sum of squares) varied by functional group (Supplemental Table B4.1). The consumption version of the model gave the best fits for benthivorous fish, planktivorous fish, and carnivorous benthos, while the base version without environmental forcing had the lowest sum of squares for piscivorous fish and the squid groups.

When assessing the impact of community composition in the first sensitivity test, the introduction of new species shifted the thermal maxima for the functional group, but, because of the cooler average Bay temperature compared to the maxima, we did not see the difference in the relative consumption curves reflected in the biomass projections (Supplemental Figure B4.1). There was limited variation in the 2054 biomasses projected under the second sensitivity test of different scaling temperatures (Supplemental Figure B4.2). The base version of the model generally had higher biomasses than those forced with temperature-dependent bioenergetics scaled to $T_{QB}$ and $T_{PB}$.

In the model versions, many of the vulnerabilities of strong predation connections for the fish groups were less than 2.0, which corresponds to bottom-up

forcing. In the third sensitivity test of changing vulnerabilities, we made these important vulnerabilities more top-down (i.e. closer to 2.0), such that the fish groups were able to further increase their consumption (Supplemental Figures B4.3-B3.5). Planktivorous fish, in particular, had higher projected biomasses when vulnerabilities were more top-down (Supplemental Figure B4.6). The smaller changes in vulnerabilities between the fitted and 20% change in vulnerabilities yielded smaller changes in biomass (Supplemental Figure B4.7).

The ActiveRespLoss is the parameter adjusted with the new respiration forcing of ForcedActresp. ActiveRespLoss is a function of total consumption, the fraction of energy devoted to respiration, and the forced respiration modifier. All model versions had an ending ActiveRespLoss higher than that of the static Ecopath model (Table 2). There were noticeable, but not strong, differences in the 2054 respiration losses, reflecting the variability of the ending respiration modifier and biomasses between model versions.

Ecosim-type models forced into the future can reach an equilibrium state if not forced by varying external drivers Therefore, the total energy inputs and outputs had nearly equilibrated by 2054 in all model versions (Supplemental Table B4.2). Given that fish groups represent just a portion of the biomass of the ecosystem, certain ecosystem metrics, such as catch, were more strongly influenced by changing fish bioenergetics than others. The respiration model versions had the highest total ecosystem respiration and the lowest overall production.

## 4. Discussion

We have expanded existing software to make a bioenergetics-based, temperature-dependent food web model and have shown that this new functionality introduced into the flexible Rpath package can impact biomass projections. Climate change elicits complex responses from organisms and ecosystems (Roessig et al., 2004), and our work adds a critical modelling component of temperature-dependent energetic losses. Our methodology can be used in combination with other tools to explore, more completely, the impacts of warming water on marine food webs.

### 4.1 Temperature

The effects of rising temperatures are increasingly being incorporated into fisheries and ecosystem models (Barange et al., 2018). Our temperature time series indicated that Narragansett Bay is likely to warm over the next few decades, similar in scale to what has been projected for other Atlantic U.S. estuaries (Muhling et al., 2018). The deterministic nature of the EwE and Rpath models allowed us to force using the average temperature trends, even though we would expect more inter-annual variability in the realized temperature. Seasonal patterns have historically varied with the winter period experiencing the greatest warming trend (Fulweiler et al., 2015), but the annual averaging of temperature was required to match the setup of the Innes-Gold et al. (2020) model. Future research could explore the spatial and temporal variability of temperature, as small-scale rates of temperature change have been shown to have physiological impacts (Peck et al., 2009).

### 4.2 Consumption thermal response

The average thermal response for a functional group can shift as community composition changes, potentially mirroring the changing temperature conditions (Flanagan et al., 2019). Warming waters can restructure marine communities as species move to remain within their preferred thermal habitat (Burrows et al., 2019; Hale et al., 2017; Nicolas et al., 2011). Our sensitivity test on changing community composition showed that large interannual variability in relative species abundance can have as strong an impact on the consumption thermal response as the introduction of new species with warmer tolerances if those new species begin at relatively small biomasses. However, we would expect the warm-water species to become more dominant over time as the environment becomes more favorable for them. Such a shift in species has been seen in Narragansett Bay over the last few decades (Collie et al., 2008; Oviatt et al., 2003). Changes in community structure could be explored further in future models that split warm and cold-water species into distinct functional groups.

### 4.3 Respiration thermal response

The Blanchard et al. (2012) parameterization of the Arrhenius equation yielded a reasonable description of changing metabolic costs for the fishes in our ecosystem. Ideally, we would have had species-specific responses, but since there were few respiration data available for the species in our ecosystem, we would have used assumed values regardless. Some studies report a temperature that corresponds to a maximum resting metabolism beyond which metabolic demand decreases (Bernreuther et al., 2013; MacIsaac et al., 1997; Schulte, 2015), but this decrease is not always seen (Giacomin et al., 2017; McKenzie et al., 2016; Stewart and

Binkowski, 1986). Other environmental drivers, such as pH, can alter the pattern of metabolic response to temperature (Schwieterman et al., 2019). Future work could assess output sensitivity to the respiration functional form chosen, and ecosystems with more metabolic studies of their component species may be amenable to responses fitted to real data.

Our ActiveRespFrac values in the base version of the model (0.48-0.61) appear reasonable, though studies are limited, and the fraction of energy devoted to respiration is not a frequently reported metric. Studies of other fishes have reported estimates varying from 26% to 70%, with more generalized studies estimating that respiratory costs constitute approximately half the energy budget (41-66%; Anacleto et al., 2018; Dabrowski, 1985; Priede, 1985; Sun et al., 2006). We strongly recommend ground truthing ActiveRespFrac values in the balancing step when building future EwE and Rpath models to be used to examine thermal drivers and bioenergetic questions. Previous work has also found that temperature altered growth rates as a result of the balance between energy inputs and outputs (Cotton et al., 2003; Gaylord et al., 2003; Present and Conover, 1992). The production curves varied between the fish groups, and the aggregation of multiple fish species with differing data quality into a single functional group response was likely responsible for any deviations in curve shape from theory.

Ecopath models are implicitly parameterized for ambient temperatures, and when the temperature changes, so will the vital parameters. The initial piscivorous fish life history parameters (i.e. *Q/B* and natural mortality) from Fishbase were generally estimated from warmer temperature environments which can result in higher

consumption and metabolism (Froese and Pauly, 2019). Creating Ecopath models can necessitate borrowing parameter values from similar species and geographic regions, but users should consider inconsistencies in environmental conditions if they hope to include temperature impacts in their modeled ecosystem.

### 4.4 Comparison of model versions

Biomass projections between the model versions were noticeably different, though these differences were small due to the consistent forcing of phytoplankton and fishing mortality stabilizing the outputs. The fish biomass projections were similar for 1994-2018 and diverged beyond 2018 as the temperature increased. The consumption versions had the highest biomasses for benthivorous and planktivorous fish reflecting the increased energy intake and assuming that all of the energy was available for production. The respiration model versions had the lowest benthivorous and planktivorous fish biomasses, a result consistent with increased energetic demands of warmer waters (Chabot et al., 2016).

Ignoring the shifting bioenergetic balance when modelling fish biomasses in response to climate change may yield optimistic forecasts for fisheries. Changing productivity of fish populations can potentially lead to lower sustainable fisheries yields (Free et al., 2019), and different management approaches may need to be considered when examining a warming ecosystem (Serpetti et al., 2017). As top predators, piscivorous fish likely had the smallest biomass differences between the respiration and consumption model versions because they were both externally forced with changing energetic demands, and their prey (i.e. the other fish groups) were also affected. In the respiration model versions, the respiration costs for piscivorous fish

were decreasing, and the group might have had higher biomasses if their prey fish had not declined due to their own increasing metabolic costs. Trophic amplification of environmental impacts has been shown in other models of warming systems, where predators showed greater declines than forced declines in primary producers because the intermediate groups were also affected (Kwiatkowski et al., 2019; Lotze et al., 2019). Even limiting variable forcing to the fish groups had trickle-down effects on other groups of the ecosystem. While the changes in the biomass of other functional groups were more minor than the fish groups, they were still noticeable which highlights the importance for bioenergetic considerations when projecting food web impacts to climate change.

The vulnerabilities estimated for our fish groups were generally bottom-up, so the predation mortality that these fish groups can exert on their prey was limited even as fish biomass increases (Christensen and Walters, 2004). Our third sensitivity tests illustrated the influence of vulnerability parameters on Ecosim and Rsim biomass projections, which has been described by others (Heymans et al., 2016; SEDAR, 2020). Because higher (i.e more top-down) vulnerabilities led to higher consumption and biomasses, top-down ecosystems may be more strongly affected by changing predator bioenergetics.

We chose to not refit the model versions (i.e. re-estimate vulnerabilities) after including the temperature drivers to isolate the impacts of changing bioenergetics. Therefore, while biomass projections differed, we did not necessarily achieve a better model fit with the inclusion of temperature-dependent fish bioenergetics. A model with vulnerabilities estimated by fitting procedures after adding the thermal responses

may better match observed biomass as has been seen in other EwE models (Bentley et al., 2020, 2017). However, our focus was on developing new metabolic functionality in Rpath and understanding the scale at which temperature-dependent fish bioenergetics can impact predicted biomasses rather than using bioenergetic theory to explain observed trends.

### 4.5 Considerations for future models

This model required a vast amount of data, but data for basic bioenergetic parameters do not always exist, particularly as studies may be biased toward species of economic importance or those able to thrive in laboratory conditions (Peck et al., 2014). Physiological studies seem to emphasize the nuance of fish response to temperature. While advanced bioenergetic models may be able to capture this nuance, generalized ecosystem modelling efforts could benefit from availability of bioenergetic data captured in standard thermal response parameters or generalized species responses. Increased ability to assess parameter uncertainty could be achieved by combining this work with the Bayesian EcoSense routine (Aydin et al., 2007), or utilizing correlation analysis (Bentley et al., 2020).

We modeled simple bioenergetic responses to temperature based on established bioenergetic principles. In reality, the factors influencing consumption and metabolism are much more complex. Thermal responses can differ between individuals as well as populations, and responses can be altered by the presence of simultaneous stressors (Farrell, 2016; Kroeker et al., 2013; Present and Conover, 1992). A more detailed base model may address the stage-specific thermal tolerances and the role of body size in metabolic performance (Hare et al., 2010; Luo and Brandt,

1993; Sibly et al., 2012), but this would require additional size- or age-specific bioenergetic data for each species. We did not include acclimation effects, though the previous thermal exposure of organisms can affect their response to temperature, nor the rate of temperature change, which can alter an organism's response (Morgan et al., 2018; Otto et al., 1976; Pinsky et al., 2020). Our work also excludes the feedbacks between temperature, reproduction, and recruitment processes (Conover and Kynard, 1981; James, 2020; Johnston et al., 1998; Pankhurst and Munday, 2011), which may be included in future models with increased use of multi-stanza groups. Finally, individual organism behavioral responses such as behavioral thermoregulation or changes in risk taking behavior were not included (Nagelkerken and Munday, 2016; Neubauer and Andersen, 2019).

Our work could be expanded in the future to include thermal responses experienced by other non-fish functional groups. Climate change has been shown to influence community composition, abundance, and timing of plankton blooms (Lawrence and Menden-Deuer, 2012; Smith et al., 2010; Sullivan et al., 2001), which could have significant feedbacks on Narragansett Bay energy flow (Monaco and Ulanowicz, 1997). Reduced primary production due to climate change could result in reduced fisheries catch if lower level production can no longer support high predator abundance (Brown et al., 2010; Cheung et al., 2011; Johansen et al., 2015). Fishing and other human activities are also considered significant drivers of ecosystem indicators (Link et al., 2010). More confidence and precision in future biomass estimates could be achieved through the inclusion of the thermal responses of the lower trophic level groups and additional varying top-down and bottom-up dynamics.

### 4.6 Conclusion

EwE has most often been used to address fisheries harvest questions (Pauly et al., 2000); our work builds on previous applications of environmentally driven food web models used to explore climate change impacts. In our Narragansett Bay case study, we have demonstrated that the inclusion of temperature-dependent bioenergetic drivers into existing Rpath and Rsim models can alter projections of biomass and energy flow. Ecosystem health and sustainability goals can be better achieved by integrating principles of conservation physiology into multispecies models to gain improved resolution on how ecosystems will respond to environmental pressures (McKenzie et al., 2016). Productivity of Narragansett Bay, or similar ecosystems, may be compromised in a warmer future if fish or other ectotherms devote greater amounts of energy towards meeting metabolic demands. Our novel methodology is intended to serve as an example to address such questions in other warming marine ecosystems (Pershing et al., 2015) or lake environments (Adrian et al., 2009) in which there may limited ability for fish to seek alternate temperatures. The new functionality for temperature-dependent respiration in the Rpath package can be combined with other thermally-driven model components to provide the most comprehensive predictions of how a food web will respond to climate change.

## 5. Acknowledgments

This work was supported by Rhode Island National Science Foundation Established Program to Stimulate Competitive Research Grant #OIA-165522. We acknowledge the World Climate Research Programme, which, through its Working Group on Coupled Modelling, coordinated and promoted CMIP6. We thank the climate modeling

groups for producing and making available their model output, the Earth System Grid Federation (ESGF) for archiving the data and providing access, and the multiple funding agencies who support CMIP6 and ESGF. We thank those that assisted with the development of this model and for their edits on this manuscript including J. Langan, C. Suckling, and R. Bell. This work is a contribution of the Rhode Island Marine Fisheries Institute.

## 6. References


Adrian, R., O'Reilly, C.M., Zagarese, H., Baines, S.B., Hessen, D.O., Keller, W., Livingstone, D.M., Sommaruga, R., Straile, D., Van Donk, E., Weyhenmeyer, G.A., Winder, M., 2009. Lakes as sentinels of climate change. Limnol. Oceanogr. 54, 2283–2297. https://doi.org/10.4319/lo.2009.54.6_part_2.2283

Ahrens, R.N.M., Walters, C.J., Christensen, V., 2012. Foraging arena theory. Fish Fish. 13, 41–59. https://doi.org/10.1111/j.1467-2979.2011.00432.x

Anacleto, P., Figueiredo, C., Baptista, M., Maulvault, A.L., Camacho, C., Pousão-Ferreira, P., Valente, L.M.P., Marques, A., Rosa, R., 2018. Fish energy budget under ocean warming and flame retardant exposure. Environ. Res. 164, 186–196. https://doi.org/10.1016/j.envres.2018.02.023

Aydin, K., Lucey, S., Gaichas, S., 2016. Rpath: R implementation of Ecopath with Ecosim.

Aydin, K.Y., Gaichas, S., Ortiz, I., Kinzey, D., Friday, N., 2007. A comparison of the Bering Sea, Gulf of Alaska, and Aleutian Islands large marine ecosystems through food web modeling. U.S. Dep. Commer., NOAA Tech. Memo. NMFS-AFSC-178 298.

Barange, Bahri, Beveridge, Cochrane, Funge-Smith, Poulain, 2018. Impacts of climate change on fisheries and aquaculture: synthesis of current knowledge, adaptation and mitigation options. Rome.

Bell, R.J., Wood, A., Hare, J., Richardson, D., Manderson, J., Miller, T., 2018. Rebuilding in the face of climate change. Can. J. Fish. Aquat. Sci. 75, 1405–1414. https://doi.org/https://doi.org/10.1139/cjfas-2017-0085

Bentley, J.W., Serpetti, N., Fox, C.J., Heymans, J.J., Reid, D.G., 2020. Retrospective analysis of the influence of environmental drivers on commercial stocks and fishing opportunities in the Irish Sea. Fish. Oceanogr. 29, 415–435. https://doi.org/10.1111/fog.12486

Bentley, J.W., Serpetti, N., Heymans, J.J., 2017. Investigating the potential impacts of ocean warming on the Norwegian and Barents Seas ecosystem using a time-dynamic food-web model. Ecol. Modell. 360, 94–107. https://doi.org/10.1016/j.ecolmodel.2017.07.002

Bernreuther, M., Herrmann, J.P., Peck, M.A., Temming, A., 2013. Growth energetics of juvenile herring, *Clupea harengus L.*: Food conversion efficiency and temperature dependency of metabolic rate. J. Appl. Ichthyol. 29, 331–340. https://doi.org/10.1111/jai.12045

Blanchard, J.L., Jennings, S., Holmes, R., Harle, J., Merino, G., Allen, J.I., Holt, J., Dulvy, N.K., Barange, M., 2012. Potential consequences of climate change for primary production and fish production in large marine ecosystems. Philos. Trans. R. Soc. B Biol. Sci. 367, 2979–2989. https://doi.org/10.1098/rstb.2012.0231

Brander, K., 2015. Improving the reliability of fishery predictions under climate change. Curr. Clim. Chang. Reports 1, 40–48. https://doi.org/10.1007/s40641-015-0005-7

Brandt, S.B., 1993. The effect of thermal fronts on fish growth: A bioenergetics evaluation of food and temperature. Estuaries 16, 142–159.

Brett, J.R., 1971. Energetic responses of salmon to temperature. A study of some thermal relations in the physiology and freshwater ecology of sockeye salmon (*Oncorhynchus nerka*). Am. Zool. 11, 99–113. https://doi.org/https://doi.org/10.1093/icb/11.1.99

Brown, C.J., Fulton, E.A., Hobday, A.J., Matear, R.J., Possingham, H.P., Bulman, C., Christensen, V., Forrest, R.E., Gehrke, P.C., Gribble, N.A., Griffiths, S.P., Lozano-Montes, H., Martin, J.M., Metcalf, S., Okey, T.A., Watson, R., Richardson, A.J., 2010. Effects of climate-driven primary production change on marine food webs: implications for fisheries and conservation. Glob. Chang. Biol. 16, 1194–1212. https://doi.org/10.1111/j.1365-2486.2009.02046.x

Brown, J.H., Gillooly, J.F., Allen, A.P., Savage, V.M., West, G.B., 2004. Toward a metabolic theory of ecology. Ecology 85, 1771–1789. https://doi.org/https://doi.org/10.1890/03-9000

Buchheister, A., Bonzek, C.F., Gartland, J., Latour, R.J., 2013. Patterns and drivers of the demersal fish community of Chesapeake Bay. Mar. Ecol. Prog. Ser. 481, 161–180. https://doi.org/doi: 10.3354/meps10253

Buchheister, A., Miller, T.J., Houde, E.D., 2017. Evaluating ecosystem-based reference points for Atlantic menhaden. Mar. Coast. Fish. 9, 457–478. https://doi.org/10.1080/19425120.2017.1360420

Buckel, J. A., Steinberg, N.D., Conover, D.O., 1995. Effects of temperature, salinity, and fish size on growth and consumption of juvenile bluefish. J. Fish Biol. 47, 696–706. https://doi.org/10.1111/j.1095-8649.1995.tb01935.x

Burrows, M.T., Bates, A.E., Costello, M.J., Edwards, M., Edgar, G.J., Fox, C.J., Halpern, B.S., Hiddink, J.G., Pinsky, M.L., Batt, R.D., García Molinos, J., Payne, B.L., Schoeman, D.S., Stuart-Smith, R.D., Poloczanska, E.S., 2019. Ocean community warming responses explained by thermal affinities and temperature gradients. Nat. Clim. Chang. https://doi.org/10.1038/s41558-019-0631-5

Chabot, D., McKenzie, D.J., Craig, J.F., 2016. Metabolic rate in fishes: definitions, methods and significance for conservation physiology. J. Fish Biol. 88, 1–9. https://doi.org/10.1111/jfb.12873

Cheung, W.W.L., Dunne, J., Sarmiento, J.L., Pauly, D., 2011. Integrating ecophysiology and plankton dynamics into projected maximum fisheries catch potential under climate change in the Northeast Atlantic. ICES J. Mar. Sci. 68, 1008–1018. https://doi.org/10.1093/icesjms/fsr012

Christensen, V., Pauly, 1992. ECOPATH II-A Software for Balancing Steady-State Ecosystem Models and Calculating Network Characteristics. Ecol. Modell. 613, 169–185. https://doi.org/10.1016/0304-3800(92)90016-8

Christensen, V., Walters, C.J., 2004. Ecopath with Ecosim: Methods, capabilities and limitations. Ecol. Modell. 172, 109–139. https://doi.org/10.1016/j.ecolmodel.2003.09.003

Christensen, V., Walters, C.J., Pauly, D., 2005. Ecopath with Ecosim: a user's guide, Fisheries Centre, University of British Columbia, Vancouver. https://doi.org/10.1016/0304-3800(92)90016-8

Christensen, V., Walters, C.J., Pauly, D., Forrest, R., 2008. Ecopath with Ecosim version 6 User Guide.

Clarke, A., Johnston, N.M., 1999. Scaling of metabolic rate with body mass and temperature in teleost fish. J. Anim. Ecol. 68, 893–905. https://doi.org/10.1046/j.1365-2656.1999.00337.x

Coll, M., Bundy, A., Shannon, L.J., 2009. Ecosystem modelling using the Ecopath with Ecosim approach, in: Megrey, B.A., Moksness, E. (Eds.), Computers in Fisheries Research. pp. 1–421. https://doi.org/10.1007/978-1-4020-8636-6

Colléter, M., Valls, A., Guitton, J., Gascuel, D., Pauly, D., Christensen, V., 2015. Global overview of the applications of the Ecopath with Ecosim modeling approach using the EcoBase models repository. Ecol. Modell. 302, 42–53. https://doi.org/10.1016/j.ecolmodel.2015.01.025

Collie, J.S., Wood, A.D., Jeffries, H.P., 2008. Long-term shifts in the species composition of a coastal fish community. Can. J. Fish. Aquat. Sci. 65, 1352–1365. https://doi.org/10.1139/F08-048

Conover, D.O., Kynard, B.E., 1981. Environmental sex determination: Interaction of temperature and genotype in a fish. Science. 213, 577–579. https://doi.org/10.1126/science.213.4507.577

Cooke, S.J., Killen, S.S., Metcalfe, J.D., McKenzie, D.J., Mouillot, D., Jørgensen, C., Peck, M.A., 2014. Conservation physiology across scales: Insights from the marine realm. Conserv. Physiol. 2, 1–15. https://doi.org/10.1093/conphys/cou024

Corrales, X., Coll, M., Ofir, E., Heymans, J.J., Steenbeek, J., Goren, M., Edelist, D., Gal, G., 2018. Future scenarios of marine resources and ecosystem conditions in the Eastern Mediterranean under the impacts of fishing, alien species and sea warming. Sci. Rep. 8, 14284. https://doi.org/10.1038/s41598-018-32666-x

Corrales, X., Coll, M., Ofir, E., Piroddi, C., Goren, M., Edelist, D., Heymans, J.J., Steenbeek, J., Christensen, V., Gal, G., 2017. Hindcasting the dynamics of an Eastern Mediterranean marine ecosystem under the impacts of multiple stressors. Mar. Ecol. Prog. Ser. 580, 17–36. https://doi.org/10.3354/meps12271

Cotton, C., Walker, R., Recicar, T., 2003. Effects of Temperature and Salinity on Growth of Juvenile Black Sea Bass, with Implications for Aquaculture. N. Am. J. Aquac. 65, 330–338. https://doi.org/10.1577/c02-037

Dabrowski, K.R., 1985. Energy Budget of Coregonid (*Coregonus* spp.) Fish Growth, Metabolism and Reproduction. Oikos 45. https://doi.org/10.2307/3565571

Dahlke, F.T., Wohlrab, S., Butzin, M., Pörtner, H.-O., 2020. Thermal bottlenecks in the life cycle define climate vulnerability of fish. Science. 369, 65–70. https://doi.org/10.1126/science.aaz3658

Dalla Via, J., Villani, P., Gasteiger, E., Niederstätter, H., 1998. Oxygen consumption in sea bass fingerling *Dicentrarchus labrax* exposed to acute salinity and temperature changes: Metabolic basis for maximum stocking density estimations. Aquaculture 169, 303–313. https://doi.org/10.1016/S0044-8486(98)00375-5

Deslauriers, D., Chipps, S.R., Breck, J.E., Rice, J.A., Madenjian, C.P., 2017. Fish Bioenergetics 4.0: An R-Based Modeling Application. Fisheries 42, 586–596. https://doi.org/10.1080/03632415.2017.1377558

Eyring, V., Bony, S., Meehl, G.A., Senior, C.A., Stevens, B., Stouffer, R.J., Taylor, K.E., 2016. Overview of the Coupled Model Intercomparison Project Phase 6 (CMIP6) experimental design and organization. Geosci. Model Dev. 9, 1937–1958. https://doi.org/10.5194/gmd-9-1937-2016

Farrell, A.P., 2016. Pragmatic perspective on aerobic scope: Peaking, plummeting, pejus and apportioning. J. Fish Biol. 88, 322–343. https://doi.org/10.1111/jfb.12789

Flanagan, P.H., Jensen, O.P., Morley, J.W., Pinsky, M.L., 2019. Response of marine communities to local temperature changes. Ecography (Cop.). 42, 214–224. https://doi.org/10.1111/ecog.03961

Fogarty, M.J., Collie, J.S., 2020. Fishery Ecosystem Dynamics, Fishery Ecosystem Dynamics. https://doi.org/10.1093/oso/9780198768937.001.0001

Free, C.M., Thorson, J.T., Pinsky, M.L., Oken, K.L., Wiedenmann, J., Jensen, O.P., 2019. Impacts of historical warming on marine fisheries production. Science. 365, 979–983. https://doi.org/10.1126/science.aau1758

Froese, F., Pauly, D., 2019. FishBase [WWW Document]. Accessed October 2020. URL http://fishbase.org/

Fry, F.E.J., 1971. The effect of environmental factors on the physiology of fish, in: Fish Physiology. Academic Press, pp. 1–98. https://doi.org/10.1016/S1546-5098(08)60146-6

Fu, S.-J., Zeng, L.-Q., Li, X.-M., Pang, X., Cao, Z.-D., Peng, J.-L., Wang, Y.-X., 2009. The behavioural, digestive and metabolic characteristics of fishes with different foraging strategies. J. Exp. Biol. 212, 2296–2302. https://doi.org/10.1242/jeb.027102

Fulweiler, R.W., Oczkowski, A.J., Miller, K.M., Oviatt, C.A., Pilson, M.E.Q., 2015. Whole truths vs. half truths - And a search for clarity in long-term water temperature records. Estuar. Coast. Shelf Sci. 157, A1–A6. https://doi.org/10.1016/j.ecss.2015.01.021

Gaylord, T.G., Schwarz, M.H., Cool, R.W., Jahncke, M.L., Craig, S.R., 2003. Thermal optima for the culture of juvenile summer flounder, *Paralichthys dentatus*. J. Appl. Aquac. 14, 155–162. https://doi.org/10.1300/J028v14n03_12

Giacomin, M., Schulte, P.M., Wood, C.M., 2017. Differential effects of temperature on oxygen consumption and branchial fluxes of urea, ammonia, and water in the dogfish shark (*Squalus acanthias suckleyi*). Physiol. Biochem. Zool. 90, 627–637. https://doi.org/10.1086/694296

Gillooly, J.F., Brown, J.H., West, G.B., Savage, V.M., Charnov, E.L., 2001. Effects of size and temperature on metabolic rate. Science. 293, 2248–2251. https://doi.org/10.1126/science.1061967

Hale, S.S., Buffum, H.W., Kiddon, J.A., Hughes, M.M., 2017. Subtidal Benthic Invertebrates Shifting Northward Along the US Atlantic Coast. Estuaries and Coasts 40, 1744–1756. https://doi.org/10.1007/s12237-017-0236-z

Hansen, P., Johnson, T., Schindler, D.E., Kitchell, J., 1997. Fish Bioenergetics 3.0 Manual. Fish Bioenerg. 3.0.

Hansson, S., Rudstam, L.G., Kitchell, J.F., Hildén, M., Johnson, B.L., Peppard, P.E., 1996. Predation rates by North Sea cod (*Gadus morhua*) - Predictions from models on gastric evacuation and bioenergetics. ICES J. Mar. Sci. 53. https://doi.org/10.1006/jmsc.1996.0010

Hare, J.A., Alexander, M.A., Fogarty, M.J., Williams, E.H., Scott, J.D., 2010. Forecasting the dynamics of a coastal fishery species using a coupled climate-population model. Ecol. Appl. 20, 452–464. https://doi.org/https://doi.org/10.1890/08-1863.1

Hartman, K.J., Brandt, S.B., 1995. Comparative energetics and the development of bioenergetics models for sympatric estuarine piscivores. Can. J. Fish. Aquat. Sci. 52, 1647–1666. https://doi.org/10.1139/f95-759

Harvey, C.J., 2009. Effects of temperature change on demersal fishes in the California Current: A bioenergetics approach. Can. J. Fish. Aquat. Sci. 66, 1449–1461. https://doi.org/10.1139/F09-087

Heymans, J.J., Coll, M., Link, J.S., Mackinson, S., Steenbeek, J., Walters, C., Christensen, V., 2016. Best practice in Ecopath with Ecosim food-web models for ecosystem-based management. Ecol. Modell. 331, 173–184. https://doi.org/10.1016/j.ecolmodel.2015.12.007

Innes-Gold, A., Heinichen, M., Gorospe, K., Truesdale, C., Collie, J., Humphries, A., 2020. Modeling 25 years of food web changes in Narragansett Bay (USA) as a tool for ecosystem-based management. Mar. Ecol. Prog. Ser. 654, 17–33. https://doi.org/10.3354/meps13505

James, K.C., 2020. Vertebral growth and band-pair deposition in sexually mature little skates *Leucoraja erinacea*: is adult band-pair deposition annual? J. Fish Biol. 96, 4–13. https://doi.org/10.1111/jfb.14141

Jobling, M., 1997. Temperature and growth: Modulation of growth rate via temperature change, in: Wood, C.M., McDonald, D.G. (Eds.), Global Warming Implications for Freshwater and Marine Fish. Cambridge University Press, pp. 225–254. https://doi.org/10.1017/CBO9780511983375

Jobling, M., 1994. Fish Bioenergetics, First edit. ed. Chapman & Hall.

Johansen, J.L., Jones, G.P., 2011. Increasing ocean temperature reduces the metabolic performance and swimming ability of coral reef damselfishes. Glob. Chang. Biol. 17, 2971–2979. https://doi.org/10.1111/j.1365-2486.2011.02436.x

Johansen, J.L., Messmer, V., Coker, D.J., Hoey, A.S., Pratchett, M.S., 2014. Increasing ocean temperatures reduce activity patterns of a large commercially important coral reef fish. Glob. Chang. Biol. 20, 1067–1074. https://doi.org/10.1111/gcb.12452

Johansen, J.L., Pratchett, M.S., Messmer, V., Coker, D.J., Tobin, A.J., Hoey, A.S., 2015. Large predatory coral trout species unlikely to meet increasing energetic demands in a warming ocean. Sci. Rep. 5, 1–8. https://doi.org/10.1038/srep13830

Johnston, I.A., Cole, N.J., Abercromby, M., Vierira, V.L.A., 1998. Embryonic temperature modulates muscle growth characteristics in larval and juvenile herring. J. Exp. Biol. 201, 623–646.

Kaschner, K., Kesner-Reyes, K., Garilao, C., Rius-Barile, J., Rees, T., Froese, R., 2019. Aquamaps: Predicted range maps for aquatic species. [WWW Document]. Accessed October 2020. URL https://www.aquamaps.org/

Kitchell, J.F., Stewart, D.J., Weininger, D., 1977. Applications of a Bioenergetics Model to Yellow Perch (*Perca flavescens*) and Walleye (*Stizostedion vitreum vitreum*). J. Fish. Res. Board Canada 34. https://doi.org/10.1139/f77-258

Kleisner, K.M., Fogarty, M.J., McGee, S., Hare, J.A., Moret, S., Perretti, C.T., Saba, V.S., 2017. Marine species distribution shifts on the U.S. Northeast Continental Shelf under continued ocean warming. Prog. Oceanogr. 153, 24–36. https://doi.org/10.1016/j.pocean.2017.04.001

Kroeker, K.J., Kordas, R.L., Crim, R., Hendriks, I.E., Ramajo, L., Singh, G.S., Duarte, C.M., Gattuso, J., 2013. Impacts of ocean acidification on marine organisms: quantifying sensitivities and interaction with warming. Glob. Chang. Biol. 19, 1884–1896. https://doi.org/10.1111/gcb.12179

Kwiatkowski, L., Aumont, O., Bopp, L., 2019. Consistent trophic amplification of marine biomass declines under climate change. Glob. Chang. Biol. 25, 218–229. https://doi.org/10.1111/gcb.14468

Langan, J., Puggioni, G., Oviatt, C., Henderson, M., Collie, J., 2021. Climate Alters the Migration Phenology of Coastal Marine Species. Mar. Ecol. Prog. Ser. 660, 1–18. https://doi.org/10.3354/meps13612

Lawrence, C., Menden-Deuer, S., 2012. Drivers of protistan grazing pressure: seasonal signals of plankton community composition and environmental conditions. Mar. Ecol. Prog. Ser. 459, 39–52. https://doi.org/https://doi.org/10.3354/meps09771

Lemoine, N.P., Burkepile, D.E., 2012. Temperature-induced mismatches between consumption and metabolism reduce consumer fitness. Ecology 93, 2483–2489. https://doi.org/10.1890/12-0375.1

Link, J.S., Yemane, D., Shannon, L.J., Coll, M., Shin, Y.-J., Hill, L., Borges, M. de F., 2010. Relating marine ecosystem indicators to fishing and environmental drivers: an elucidation of contrasting responses. ICES J. Mar. Sci. 67, 787–795. https://doi.org/10.1093/icesjms/fsp258

Lotze, H.K., Tittensor, D.P., Bryndum-Buchholz, A., Eddy, T.D., Cheung, W.W.L., Galbraith, E.D., Barange, M., Barrier, N., Bianchi, D., Blanchard, J.L., Bopp, L., Büchner, M., Bulman, C.M., Carozza, D.A., Christensen, V., Coll, M., Dunne, J.P., Fulton, E.A., Jennings, S., Jones, M.C., Mackinson, S., Maury, O., Niiranen, S., Oliveros-Ramos, R., Roy, T., Fernandes, J.A., Schewe, J., Shin, Y.J., Silva, T.A.M., Steenbeek, J., Stock, C.A., Verley, P., Volkholz, J., Walker, N.D., Worm, B., 2019. Global ensemble projections reveal trophic amplification of ocean biomass declines with climate change. Proc. Natl. Acad. Sci. U. S. A. 116, 12907–12912. https://doi.org/10.1073/pnas.1900194116

Lucey, S.M., Gaichas, S.K., Aydin, K.Y., 2020. Conducting reproducible ecosystem modeling using the open source mass balance model Rpath. Ecol. Modell. 427, 109057. https://doi.org/10.1016/j.ecolmodel.2020.109057

Luo, J., Brandt, S.B., 1993. Bay anchovy Anchoa mitchilli production and consumption in mid- Chesapeake Bay based on a bioenergetics model and acoustic measures of fish abundance. Mar. Ecol. Prog. Ser. 98, 223–236. https://doi.org/10.3354/meps098223

MacIsaac, P.F., Goff, G.P., Speare, D.J., 1997. Comparison of routine oxygen consumption rates of three species of pleuronectids at three temperatures. J. Appl. Ichthyol. 13, 171–176. https://doi.org/10.1111/j.1439-0426.1997.tb00117.x

McKenzie, D.J., Axelsson, M., Chabot, D., Claireaux, G., Cooke, S.J., Corner, R.A., De Boeck, G., Domenici, P., Guerreiro, P.M., Hamer, B., Jørgensen, C., Killen, S.S., Lefevre, S., Marras, S., Michaelidis, B., Nilsson, G.E., Peck, M.A., Perez-Ruzafa, A., Rijnsdorp, A.D., Shiels, H.A., Steffensen, J.F., Svendsen, J.C., Svendsen, M.B.S., Teal, L.R., van der Meer, J., Wang, T., Wilson, J.M., Wilson, R.W., Metcalfe, J.D., 2016. Conservation physiology of marine fishes: state of the art and prospects for policy. Conserv. Physiol. 4, cow046. https://doi.org/10.1093/conphys/cow046

Monaco, M.E., Ulanowicz, R.E., 1997. Comparative ecosystem trophic structure of three U.S. mid-Atlantic estuaries. Mar. Ecol. Prog. Ser. 161, 239–254. https://doi.org/10.3354/meps161239

Morgan, R., Finnøen, M.H., Jutfelt, F., 2018. CTmax is repeatable and doesn't reduce growth in zebrafish. Sci. Rep. 8, 1–8. https://doi.org/10.1038/s41598-018-25593-4

Muhling, B.A., Gaitán, C.F., Stock, C.A., Saba, V.S., Tommasi, D., Dixon, K.W., 2018. Potential Salinity and Temperature Futures for the Chesapeake Bay Using a Statistical Downscaling Spatial Disaggregation Framework. Estuaries and Coasts 41, 349–372. https://doi.org/10.1007/s12237-017-0280-8

Nagelkerken, I., Munday, P.L., 2016. Animal behaviour shapes the ecological effects of ocean acidification and warming: Moving from individual to community-level responses. Glob. Chang. Biol. 22, 974–989. https://doi.org/10.1111/gcb.13167

Nelson, G.A., Armstrong, M.P., Stritzel-Thomson, J., Friedland, K.D., 2010. Thermal habitat of striped bass (*Morone saxatilis*) in coastal waters of northern Massachusetts, USA, during summer. Fish. Oceanogr. 19, 370–381. https://doi.org/10.1111/j.1365-2419.2010.00551.x

Neubauer, P., Andersen, K.H., 2019. Thermal performance of fish is explained by an interplay between physiology, behaviour and ecology. Conserv. Physiol. 7, 1–14. https://doi.org/10.1093/conphys/coz025

Nicolas, D., Chaalali, A., Drouineau, H., Lobry, J., Uriarte, A., Borja, A., Boët, P., 2011. Impact of global warming on European tidal estuaries: Some evidence of northward migration of estuarine fish species. Reg. Environ. Chang. 11, 639–649. https://doi.org/10.1007/s10113-010-0196-3

Nowicki, J.P., Miller, G.M., Munday, P.L., 2012. Interactive effects of elevated temperature and CO2 on foraging behavior of juvenile coral reef fish. J. Exp. Mar. Bio. Ecol. 412, 46–51. https://doi.org/10.1016/j.jembe.2011.10.020

O'Neill, B.C., Tebaldi, C., Van Vuuren, D.P., Eyring, V., Friedlingstein, P., Hurtt, G., Knutti, R., Kriegler, E., Lamarque, J.F., Lowe, J., Meehl, G.A., Moss, R., Riahi, K., Sanderson, B.M., 2016. The Scenario Model Intercomparison Project (ScenarioMIP) for CMIP6. Geosci. Model Dev. 9, 3461–3482. https://doi.org/10.5194/gmd-9-3461-2016

Olla, B., Studholme, A., Bejda, A., 1985. Behavior of juvenile bluefish *Pomatomus saltatrix* in vertical thermal gradients: influence of season, temperature acclimation and food. Mar. Ecol. Prog. Ser. 23, 165–177. https://doi.org/10.3354/meps023165

Otto, R.G., Kitchel, M.A., Rice, J.O., 1976. Lethal and Preferred Temperatures of the Alewife (*Alosa pseudoharengus*) in Lake Michigan. Trans. Am. Fish. Soc. 105, 96–106. https://doi.org/10.1577/1548-8659(1976)105<96:laptot>2.0.co;2

Pankhurst, N.W., Munday, P.L., 2011. Effects of climate change on fish reproduction and early life history stages. Mar. Freshw. Res. 62, 1015–1026. https://doi.org/10.1071/MF10269

Pauly, Daniel, Christensen, V., Walters, Carl, Pauly, D, Walters, C, 2000. Ecopath, Ecosim, and Ecospace as tools for evaluating ecosystem impact of fisheries. ICES J. Mar. Sci. 57, 697–706. https://doi.org/10.1006/jmsc.2000.0726

Peck, L.S., 2011. Organisms and responses to environmental change. Mar. Genomics 4, 237–243. https://doi.org/10.1016/j.margen.2011.07.001

Peck, L.S., Clark, M.S., Morley, S.A., Massey, A., Rossetti, H., 2009. Animal temperature limits and ecological relevance: Effects of size, activity and rates of change. Funct. Ecol. 23, 248–256. https://doi.org/10.1111/j.1365-2435.2008.01537.x

Peck, L.S., Morley, S.A., Richard, J., Clark, M.S., 2014. Acclimation and thermal tolerance in Antarctic marine ectotherms. J. Exp. Biol. 217, 16–22. https://doi.org/10.1242/jeb.089946

Pershing, A.J., Alexander, M.A., Hernandez, C.M., Kerr, L.A., Le Bris, A., 2015. Slow adaptation in the face of rapid warming leads to collapse of the Gulf of Maine cod fishery. Science. 350, 809–812. https://doi.org/10.1126/science.aac9819

Pinsky, M.L., Selden, R.L., Kitchel, Z.J., 2020. Climate-driven shifts in marine species ranges: scaling from organisms to communities. Ann. Rev. Mar. Sci. 12, 153–179. https://doi.org/10.1146/annurev-marine-010419

Polovina, J.J., 1984. Model of a coral reef ecosystem - I. The ecopath model and its application to French Frigate Shoals. Coral Reefs 3, 1–11. https://doi.org/10.1007/BF00306135

Present, T.M.C., Conover, D.O., 1992. Physiological Basis of Latitudinal Growth Differences in *Menidia menidia*: Variation in Consumption or Efficiency? Funct. Ecol. 6, 23–31.

Priede, I.G., 1985. Metabolic Scope in Fishes, in: Fish Energetics. pp. 33–64. https://doi.org/10.1007/978-94-011-7918-8_2

R Core Team, 2019. R: A Language and Environment for Statistical Computing.

Ries, R., Perry, S., 1995. Potential effects of global climate warming on brook trout growth and prey consumption in central Appalachian streams, USA. Clim. Res. 5, 197–206. https://doi.org/10.3354/cr005197

Roessig, J.M., Woodley, C.M., Cech, J.J., Hansen, L.J., 2004. Effects of global climate change on marine and estuarine fishes and fisheries. Rev. Fish Biol. Fish. 14, 251–275.

Sandersfeld, T., Mark, F.C., Knust, R., 2017. Temperature-dependent metabolism in Antarctic fish: Do habitat temperature conditions affect thermal tolerance ranges? Polar Biol. 40, 141–149. https://doi.org/10.1007/s00300-016-1934-x

Schulte, P.M., 2015. The effects of temperature on aerobic metabolism: Towards a mechanistic understanding of the responses of ectotherms to a changing environment. J. Exp. Biol. 218, 1856–1866. https://doi.org/10.1242/jeb.118851

Schwieterman, G.D., Crear, D.P., Anderson, B.N., Lavoie, D.R., Sulikowski, J.A., Bushnell, P.G., Brill, R.W., 2019. Combined effects of acute temperature change and elevated pCO2 on the metabolic rates and hypoxia tolerances of clearnose skate (*Rostaraja eglanteria*), summer flounder (*Paralichthys dentatus*), and thorny skate (*Amblyraja radiata*). Biology (Basel). 8. https://doi.org/10.3390/biology8030056

SEDAR, 2020. Atlantic Menhaden Ecological Reference Points Stock Assessment Report, SEDAR 69. North Charleston, SC.

Serpetti, N., Baudron, A.R., Burrows, M.T., Payne, B.L., Helaouët, P., Fernandes, P.G., Heymans, J.J., 2017. Impact of ocean warming on sustainable fisheries management informs the Ecosystem Approach to Fisheries. Sci. Rep. 7, 1–15. https://doi.org/10.1038/s41598-017-13220-7

Sibly, R.M., Brown, J.H., Kodric-Brown, A., 2012. Metabolic Ecology: A Scaling Approach, First Edit. ed. John Wiley & Sons, Ltd. https://doi.org/10.1002/9781119968535

Slesinger, E., Andres, A., Young, R., Seibel, B., Saba, V., Phelan, B., Rosendale, J., Wieczorek, D., Saba, G., 2019. The effect of ocean warming on black sea bass (*Centropristis striata*) aerobic scope and hypoxia tolerance. PLoS One 14, e0218390. https://doi.org/10.1371/journal.pone.0218390

Smith, L.M., Whitehouse, S., Oviatt, C.A., 2010. Impacts of climate change on Narragansett Bay. Northeast. Nat. 17, 77–90. https://doi.org/10.1656/045.017.0106

Stewart, D.J., Binkowski, F.P., 1986. Dynamics of Consumption and Food Conversion by Lake Michigan Alewives: An Energetics-Modeling Synthesi. Trans. Am. Fish. Soc. 115, 643–661.

Sullivan, B.K., Van Keuren, D., Clancy, M., 2001. Timing and size of blooms of the ctenophore *Mnemiopsis leidyi* in relation to temperature in Narragansett Bay, RI, Hydrobiologia.

Sun, L., Chen, H., Huang, L., 2006. Effect of temperature on growth and energy budget of juvenile cobia (*Rachycentron canadum*). Aquaculture 261, 872–878. https://doi.org/10.1016/j.aquaculture.2006.07.028

University of Rhode Island Graduate School of Oceanography, 2021. Fish trawl methods. [WWW Document]. Accessed March 2021. URL https://web.uri.edu/gso/research/fish-trawl/methods/

Villasante, S., Arreguín-Sánchez, F., Heymans, J.J., Libralato, S., Piroddi, C., Christensen, V., Coll, M., 2016. Modelling marine ecosystems using the Ecopath with Ecosim food web approach: New insights to address complex dynamics after 30 years of developments. Ecol. Modell. 331, 1–4. https://doi.org/10.1016/j.ecolmodel.2016.04.017

Volkoff, H., Rønnestad, I., 2020. Effects of temperature on feeding and digestive processes in fish. Temperature 7, 307–320. https://doi.org/10.1080/23328940.2020.1765950

Walters, C., Christensen, V., 2007. Adding realism to foraging arena predictions of trophic flow rates in Ecosim ecosystem models: Shared foraging arenas and bout feeding. Ecol. Modell. 209, 342–350. https://doi.org/10.1016/j.ecolmodel.2007.06.025

## 7. Tables

Table 1: Naming convention and descriptions of the base and temperature-dependent versions of the Rpath implementation of the Narragansett Bay food web model.

| Model Version | Description | Scenarios Run |
|---|---|---|
| Base | Rsim translation of Innes-Gold et al. (2020) Ecosim model. Model version used the same fishing and biomass forcing as the Ecosim model. No environmental forcing was included in the 1994-2054 projection. | N/A |
| Consumption (Cons) | Built on the base version of model run with temperature-dependent consumption only. Consumption modifiers applied using the ForcedSearch function. Observed temperatures used for the 1994-2018 projections. | Two runs from 2019-2054: High warming & Low Warming |
| Respiration (Resp) | Built on the consumption version of the model run with temperature-dependent respiration. Respiration modifiers applied using the new ForcedActresp function. Observed temperatures used for the 1994-2018 projections. | Two runs from 2019-2054: High warming & Low Warming |

Table 2: Biomass, the fraction of energy towards respiration (ActiveRespFrac), and the energy lost to respiration (ActiveRespLoss) for all model versions including the static Rpath starting point for the dynamic versions. High is the high warming temperature forcing scenario, and Low is low warming scenario. In the respiration versions, the ActiveRespFrac is shown with the forced respiration modifier in parentheses. For the dynamic models, the value shown is the 2054 projection.

| Functional group | Variable | Base | Cons High | Cons Low | Resp High | Resp Low | Rpath |
|---|---|---|---|---|---|---|---|
| Plank-tivorous Fish | Annual_Biomass | 15.28 | 17.03 | 16.53 | 14.55 | 14.71 | 12.3 |
| | ActiveRespFrac | 0.53 | 0.53 | 0.53 | 0.53 (1.042) | 0.53 (1.035) | 0.53 |
| | ActiveRespLoss | 76.30 | 81.12 | 80.13 | 81.44 | 80.69 | 71.14 |
| Benth-ivorous Fish | Annual_Biomass | 10.28 | 12.46 | 11.90 | 9.93 | 10.08 | 9.22 |
| | ActiveRespFrac | 0.61 | 0.61 | 0.61 | 0.61 (1.035) | 0.61 (1.030) | 0.61 |
| | ActiveRespLoss | 31.51 | 36.14 | 35.27 | 34.39 | 34.10 | 25.31 |
| Pisc-ivorous Fish | Annual_Biomass | 6.63 | 8.25 | 7.78 | 9.25 | 8.57 | 2.08 |
| | ActiveRespFrac | 0.48 | 0.48 | 0.48 | 0.48 (0.924) | 0.48 (0.932) | 0.48 |
| | ActiveRespLoss | 8.42 | 10.20 | 9.81 | 9.45 | 9.18 | 4.61 |

## 8. Figures

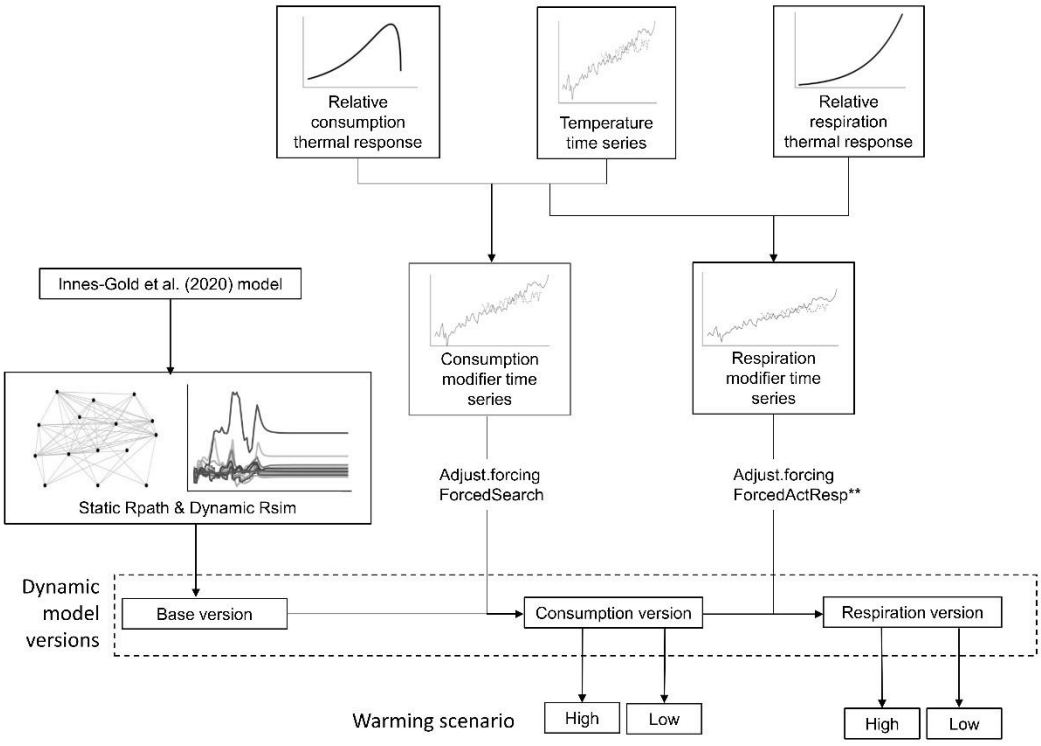


Figure 1: Conceptual diagram for the inclusion of temperature-dependent bioenergetics into an Rpath with Rsim model. Adjust.forcing is the function used to modify the specified parameter in the temperature-dependent model versions. This work introduces the ability to adjust ForcedActresp.

.

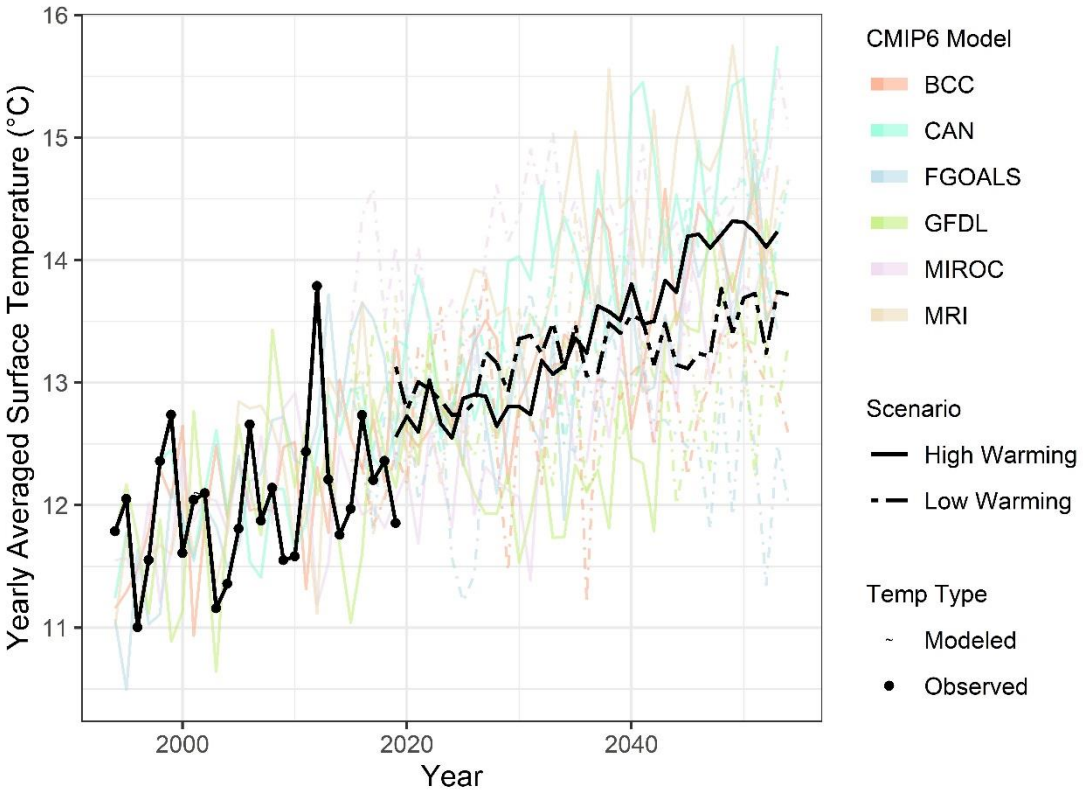


Figure 2: Temperature time series inputs for the temperature-dependent model versions. The black line with points between 1994 and 2018 is the observed yearly average surface temperature of the GSO Fox Island fish trawl station. The colored lines are the six CMIP6 models. Solid lines are the high warming scenario and the dashed are the low warming scenarios. The projected Bay surface temperatures for high warming (solid black line) and low warming (dashed black line) are the means of the six CMIP6 models. A table showing the values of the final temperature time series can be found in Supplemental Table B1.1.

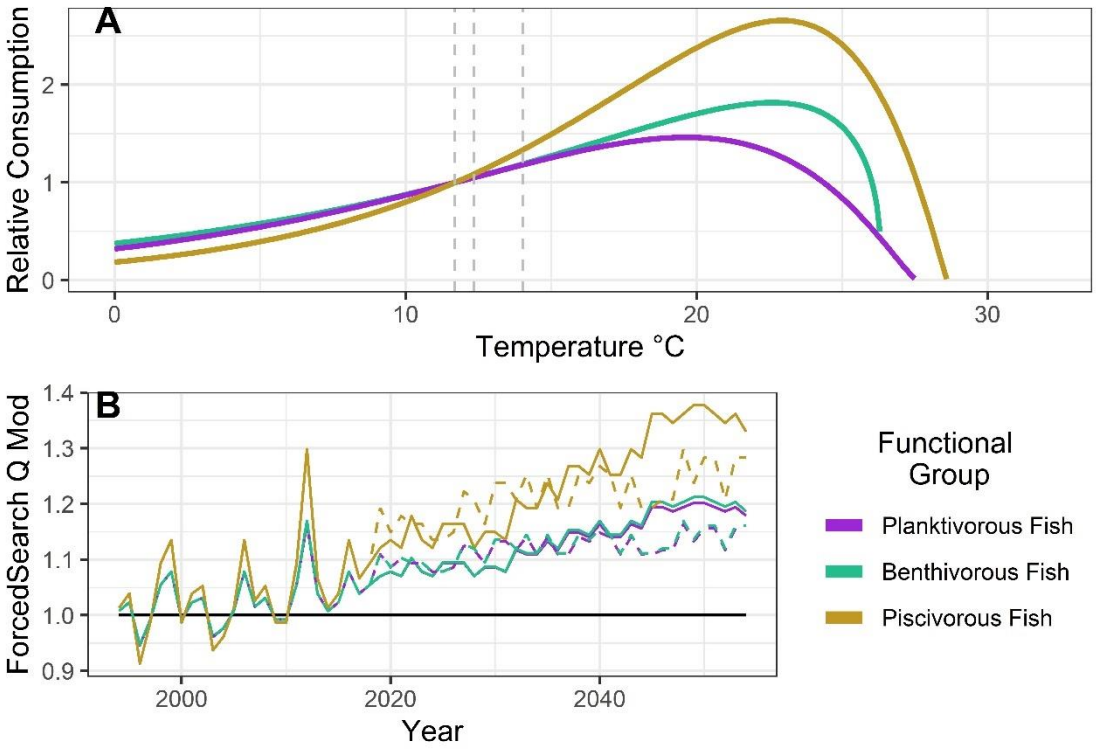


Figure 3: A) The relative consumption curves by functional group in response to temperature. Vertical grey dashed lines have been added to show $T_{B94}$, the 2018 observed average temperature, and the 2054 average temperature as projected under the high warming scenario. B) The consumption modifier time series applied to ForcedSearch in the temperature-dependent versions of the model. Beyond 2018, the solid line is the modifier in response to the high warming scenario and the dashed lines reflect the low warming scenario. The default ForcedSearch of the base model is 1.0, shown by a black line.

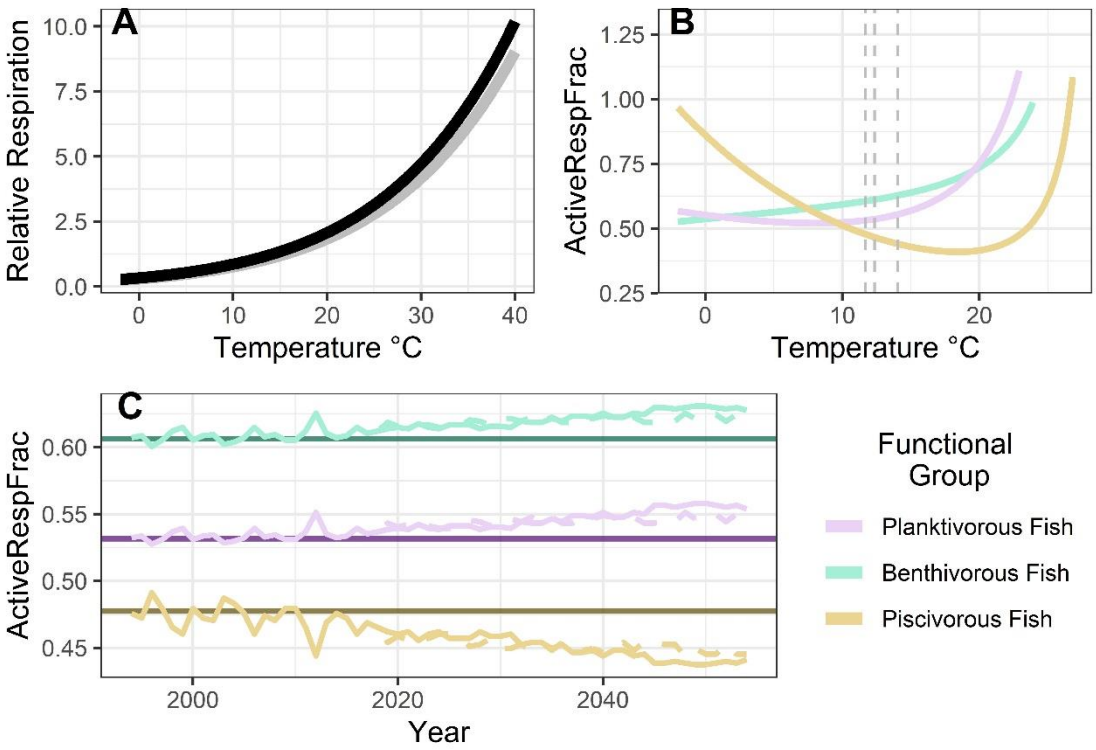


Figure 4: A) The relative respiration curves (black) compared to the original Blanchard curve (grey). B) ActiveRespFrac (i.e. Rpath parameter value representing fraction of energy devoted to respiratory costs) by temperature for each functional group, as calculated from total respiration divided by total consumption. Vertical grey dashed lines have been added to show $T_{B94}$, the 2018 observed average temperature, and the 2054 average temperature as projected under the high warming scenario. C) ActiveRespFrac as a time series. The horizontal dark lines show the static ActiveRespFrac of the base version of the model. The solid pale lines after 2018 show the ActiveRespFrac in the high warming scenario and the dashed lines are for the low warming scenario.

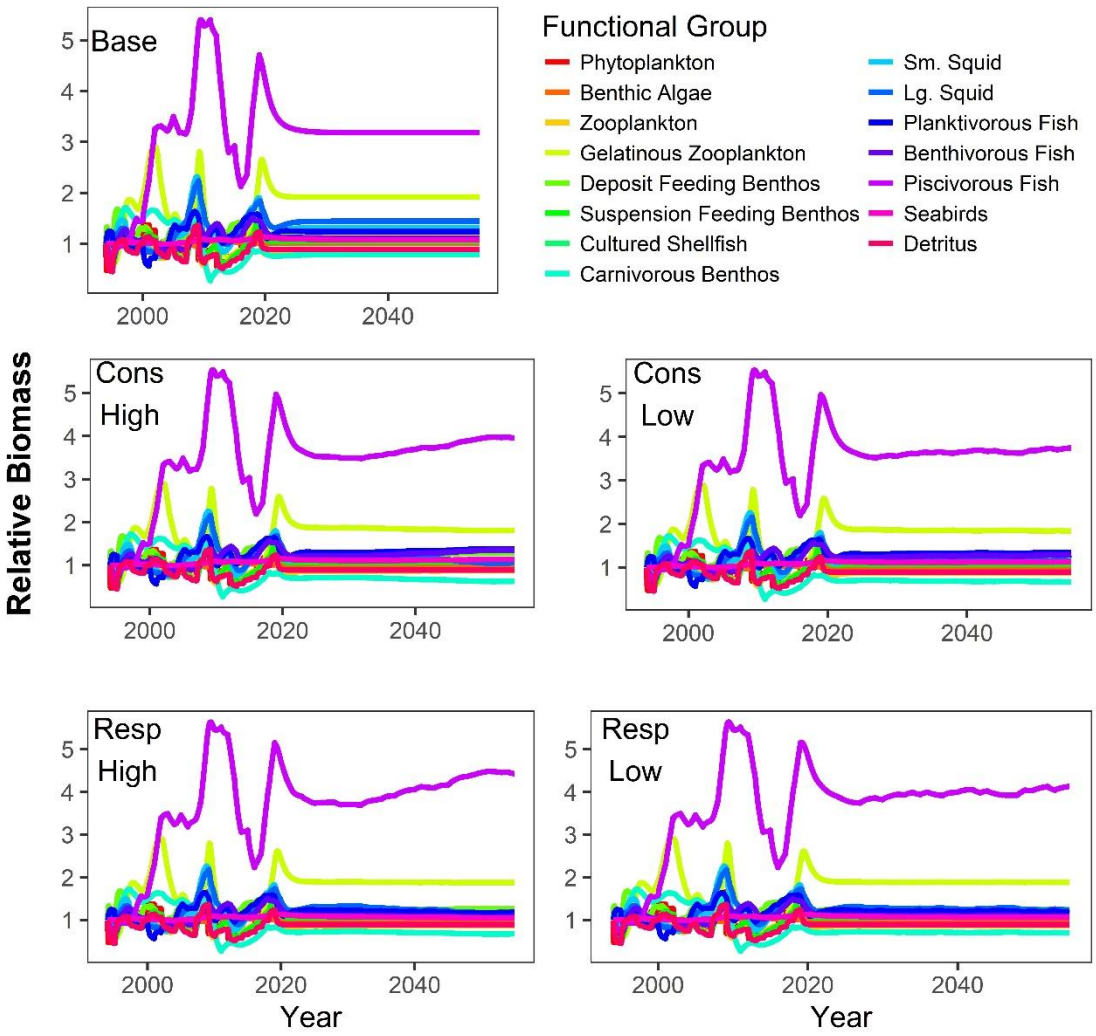


Figure 5: Rsim relative biomass outputs compared to the Rpath starting biomasses for the three model versions and two warming scenarios. The cultured shellfish group is not included in these plots. The forced biomass of the cultured shellfish group increases by orders of magnitude, so the relative biomass scaling for that group does not align with the others.

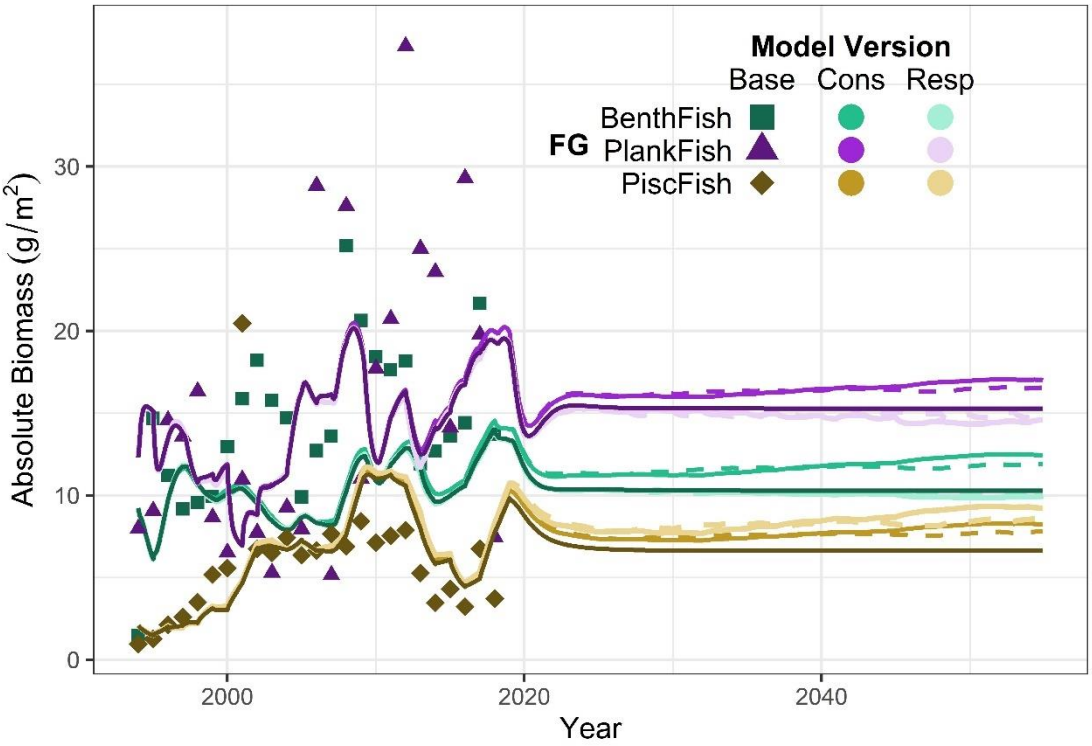


Figure 6: Biomass trajectories (lines) for the fish functional groups (FG) compared to the observed time series (points) used by Innes-Gold et al. (2020) to fit the original Ecosim model. Colors represent the model version and line type indicates the warming scenario. Solid lines beyond 2018 show both the base model version without temperature-dependence and the consumption and respiration model versions run with the high warming scenario. Dashed lines show the low warming scenario.

## SUPPORTING INFORMATION

### Appendix A. Supplementary Methods

*Supplement 1: Base model inputs*

The input parameters between Ecopath and Rpath were nearly the same. To best match outputs between the Rpath and Ecopath software, the Rpath stanza function was adjusted so that Von Bertalanffy maximum age was 0.9 * Weight infinity ($W_{inf}$), as opposed to 0.99 * $W_{inf}$. Additionally, for the Rsim dynamics, detritus *P/B* needs to be entered instead of biomass. However, Rsim detritus projection did not match those of Ecosim, so the *P/B* value of 741 was chosen based on the sum of squares best fit between the Rsim predicted detrital biomass and the Ecosim modeled biomass. The detritus B_BaseRef, or reference biomass, parameter of Rsim was changed to 3.866 to match the EwE initial biomass. The forcing functions of fishing mortality, phytoplankton biomass, and cultured shellfish biomass remained the same as those used by Innes-Gold et al. (2020). The static, Ecosim-estimated fishing mortality of suspension feeding benthos was also included in the Rsim forcing. The original Ecosim model was fitted with biomass time series for the upper trophic level groups; the Rsim model was not refitted and used the same input parameters (i.e. vulnerabilities) as Ecosim. The Rsim dynamic simulations were integrated with the Adams-Bashforth (AB) method.

Supplemental Table A1.1: Functional group codes and names as in the Rpath model versions.

| **Functional Group** | **FG Code** |
|---|---|
| Outside | 0 |
| Phytoplankton | 1 |
| Benthic Algae | 2 |
| Zooplankton | 3 |
| Gelatinous Zooplankton | 4 |
| Deposit Feeding Benthos | 5 |
| Suspension Feeding Benthos | 6 |
| Cultured Shellfish | 7 |
| Carnivorous Benthos | 8 |
| Small Squid | 9 |
| Large Squid | 10 |
| Planktivorous Fish | 11 |
| Benthivorous Fish | 12 |
| Piscivorous Fish | 13 |
| Seabirds | 14 |
| Detritus | 15 |

Supplemental Table A1.2. The fish functional groups consist of species deemed to be of commercial, recreational, or ecological importance in Narragansett Bay. Species were taken from Innes-Gold et al. (2020).

| Functional Group | Species Included (Common) | Scientific Name |
|---|---|---|
| Planktivorous Fish | Atlantic menhaden | *Brevoortia tyannus* |
| | Atlantic moonfish | *Selene setapinnis* |
| | Alewife | *Alosa pseudoharengus* |
| | Bay anchovy | *Anchoa mitchilli* |
| | Atlantic silverside | *Menidia menidia* |
| | Atlantic herring | *Clupea harengus* |
| | Butterfish | *Peprilus triacanthus* |
| | Blueback herring | *Alosa aestivalis* |
| Benthivorous Fish | Winter flounder | *Pleuronectes americanus* |
| | Tautog | *Tautoga onitis* |
| | Scup | *Stenotomus chrysops* |
| | Black sea bass | *Centropristis striata* |
| | Little skate | *Laucoraja erinacea* |
| | Striped searobin | *Prionotus evolans* |
| Piscivorous Fish | Summer flounder | *Paralichthys dentatus* |
| | Atlantic striped bass | *Morone saxatilis* |
| | Bluefish | *Pomatomus saltatrix* |
| | Weakfish | *Cynoscion regalis* |
| | Spiny dogfish | *Squalus acanthias* |

*Supplement 2: Temperature*

The six CMIP6 models for both the high and low warming scenarios were chosen based on the available CMIP6 updates to CMIP5 models used by Bell et al. (2018) (Supplemental Table A2.1).

Supplemental Table A2.1: Model details of the chosen Coupled Model Intercomparison Project Phase 6 (CMIP6) models used to create the high and low warming scenarios for Narragansett Bay. The model files are given as the .nc files taken from the CMIP6 data search site https://esgf-node.llnl.gov/projects/cmip6/.

| CMIP6 Model | Institution | Experiment | Citation |
|---|---|---|---|
| | BCC | | |
| Medium-Resolution Climate System Model Version 2 | Beijing Climate Center, Beijing 100081, China (BCC) | Historical<br>SSP1–2.6<br>SSP5–8.5 | Wu et al. (2018)<br>Xin et al. (2019a)<br>Xin et al. (2019b) |
| tas_Amon_BCC-CSM2-MR_historical_r1i1p1f1_gn_185001-201412.nc<br>tas_Amon_BCC-CSM2-MR_ssp126_r1i1p1f1_gn_201501-210012.nc<br>tas_Amon_BCC-CSM2-MR_ssp585_r1i1p1f1_gn_201501-210012.nc | | | |
| | CAN | | |
| Canadian Earth System Model Version 5 | Canadian Centre for Climate Modelling and Analysis, Environment and Climate Change Canada, Victoria, BC V8P 5C2, Canada (CCCma) | Historical<br>SSP1–2.6<br>SSP5–8.5 | Swart et al. (2019b)<br>Swart et al. (2019c)<br>Swart et al. (2019a) |
| tas_Amon_CanESM5_historical_r1i1p1f1_gn_185001-201412.nc<br>tas_Amon_CanESM5_ssp126_r1i1p1f1_gn_201501-210012.nc<br>tas_Amon_CanESM5_ssp585_r1i1p1f1_gn_201501-210012.nc | | | |

Continued on next page.

Supplemental Table A2.1 continued

| CMIP6 Model | Institution | Experiment | Citation |
|---|---|---|---|
| | FGOALS | | |
| Flexible Global Ocean–Atmosphere–Land System Model: Grid-Point Version 3 | Chinese Academy of Sciences, Beijing 100029, China (CAS) | Historical<br>SSP1–2.6<br>SSP5–8.5 | Li (2019a)<br>Li (2019b)<br>Li (2019c) |
| tas_Amon_FGOALS-g3_historical_r1i1p1f1_gn_199001-199912.nc<br>tas_Amon_FGOALS-g3_historical_r1i1p1f1_gn_200001-200912.nc<br>tas_Amon_FGOALS-g3_historical_r1i1p1f1_gn_201001-201612.nc<br>tas_Amon_FGOALS-g3_ssp126_r1i1p1f1_gn_201501-201912.nc<br>tas_Amon_FGOALS-g3_ssp126_r1i1p1f1_gn_202001-202912.nc<br>tas_Amon_FGOALS-g3_ssp126_r1i1p1f1_gn_203001-203912.nc<br>tas_Amon_FGOALS-g3_ssp126_r1i1p1f1_gn_204001-204912.nc<br>tas_Amon_FGOALS-g3_ssp126_r1i1p1f1_gn_205001-205912.nc<br>tas_Amon_FGOALS-g3_ssp585_r1i1p1f1_gn_201501-201912.nc<br>tas_Amon_FGOALS-g3_ssp585_r1i1p1f1_gn_202001-202912.nc<br>tas_Amon_FGOALS-g3_ssp585_r1i1p1f1_gn_203001-203912.nc<br>tas_Amon_FGOALS-g3_ssp585_r1i1p1f1_gn_204001-204912.nc<br>tas_Amon_FGOALS-g3_ssp585_r1i1p1f1_gn_205001-205912.nc | | | |
| | GFDL | | |
| Earth System Model Version 4 | National Oceanic and Atmospheric Administration, Geophysical Fluid Dynamics Laboratory, Princeton, NJ 08540, USA (NOAA-GFDL) | Historical<br>SSP1–2.6<br>SSP5–8.5 | Krasting et al. (2018)<br>John et al. (2018a)<br>John et al. (2018b) |
| tas_Amon_GFDL-ESM4_historical_r1i1p1f1_gr1_195001-201412.nc<br>tas_Amon_GFDL-ESM4_ssp126_r1i1p1f1_gr1_201501-210012.nc<br>tas_Amon_GFDL-ESM4_ssp585_r1i1p1f1_gr1_201501-210012.nc | | | |

Continued on next page.

Supplemental Table A2.1 continued

| CMIP6 Model | Institution | Experiment | Citation |
|---|---|---|---|
| | MIROC | | |
| Model for Interdisciplinary Research on Climate Version 6 | Japan Agency for Marine-Earth Science and Technology, Kanagawa 236-0001, Japan (JAMSTEC); Atmosphere and Ocean Research Institute, The University of Tokyo, Chiba 277-8564, Japan (AORI); National Institute for Environmental Studies, Ibaraki 305-8506, Japan (NIES); RIKEN Center for Computational Science, Hyogo 650-0047, Japan (R-CCS) | Historical<br>SSP1–2.6<br>SSP5–8.5 | Tatebe & Watanabe (2018)<br>Shiogama et al. (2019a)<br>Shiogama et al. (2019b) |
| tas_Amon_MIROC6_historical_r1i1p1f1_gn_195001-201412.nc<br>tas_Amon_MIROC6_ssp126_r1i1p1f1_gn_201501-210012.nc<br>tas_Amon_MIROC6_ssp585_r1i1p1f1_gn_201501-210012.nc | | | |
| | MRI | | |
| Earth System Model Version 2.0 | Meteorological Research Institute, Tsukuba, Ibaraki 305-0052, Japan (MRI) | Historical<br>SSP1–2.6<br>SSP5–8.5 | Yukimoto et al. (2019a)<br>Yukimoto et al. (2019b)<br>Yukimoto et al. (2019c) |
| tas_Amon_MRI-ESM2-0_historical_r1i1p1f1_gn_185001-201412.nc<br>tas_Amon_MRI-ESM2-0_ssp126_r1i1p1f1_gn_201501-210012.nc<br>tas_Amon_MRI-ESM2-0_ssp585_r1i1p1f1_gn_201501-210012.nc | | | |

CMIP Model Citations

John, Jasmin G; Blanton, Chris; McHugh, Colleen; Radhakrishnan, Aparna; Rand, Kristopher; Vahlenkamp, Hans; Wilson, Chandin; Zadeh, Niki T.; Gauthier, Paul PG; Dunne, John P.; Dussin, Raphael; Horowitz, Larry W.; Lin, Pu; Malyshev, Sergey; Naik, Vaishali; Ploshay, Jeffrey; Silvers, Levi; Stock, Charles; Winton, Michael; Zeng, Yujin (2018a). NOAA-GFDL GFDL-ESM4 model output prepared for CMIP6 ScenarioMIP ssp126. Version 20180701.Earth System Grid Federation. https://doi.org/10.22033/ESGF/CMIP6.8684

John, Jasmin G; Blanton, Chris; McHugh, Colleen; Radhakrishnan, Aparna; Rand, Kristopher; Vahlenkamp, Hans; Wilson, Chandin; Zadeh, Niki T.; Gauthier, Paul PG; Dunne, John P.; Dussin, Raphael; Horowitz, Larry W.; Lin, Pu; Malyshev, Sergey; Naik, Vaishali; Ploshay, Jeffrey; Silvers, Levi; Stock, Charles; Winton, Michael; Zeng, Yujin (2018b). NOAA-GFDL GFDL-ESM4 model output prepared for CMIP6 ScenarioMIP ssp585. Version 20180701. Earth System Grid Federation. https://doi.org/10.22033/ESGF/CMIP6.8706

Krasting, John P.; John, Jasmin G; Blanton, Chris; McHugh, Colleen; Nikonov, Serguei; Radhakrishnan, Aparna; Rand, Kristopher; Zadeh, Niki T.; Balaji, V; Durachta, Jeff; Dupuis, Christopher; Menzel, Raymond; Robinson, Thomas; Underwood, Seth; Vahlenkamp, Hans; Dunne, Krista A.; Gauthier, Paul PG; Ginoux, Paul; Griffies, Stephen M.; Hallberg, Robert; Harrison, Matthew; Hurlin, William; Malyshev, Sergey; Naik, Vaishali; Paulot, Fabien; Paynter, David J; Ploshay, Jeffrey; Schwarzkopf, Daniel M; Seman, Charles J; Silvers, Levi; Wyman, Bruce; Zeng, Yujin; Adcroft, Alistair; Dunne, John P.; Dussin, Raphael; Guo, Huan; He, Jian; Held, Isaac M; Horowitz, Larry W.; Lin, Pu; Milly, P.C.D; Shevliakova, Elena; Stock, Charles; Winton, Michael; Xie, Yuanyu; Zhao, Ming (2018). NOAA-GFDL GFDL-ESM4 model output prepared for CMIP6 CMIP historical. Version 20190726. Earth System Grid Federation. https://doi.org/10.22033/ESGF/CMIP6.8597

Li L (2019a) CAS FGOALS-g3 model output prepared for CMIP6 CMIP historical. Version 20190818. Earth System Grid Federation. http://doi.org/10.22033/ESGF/CMIP6.3356

Li L (2019b) CAS FGOALS-g3 model output prepared for CMIP6 ScenarioMIP ssp126. Version 20200927. Earth System Grid Federation. http://doi.org/10.22033/ESGF/CMIP6.3465

Li L (2019c) CAS FGOALS-g3 model output prepared for CMIP6 ScenarioMIP ssp585. Version 20190818. Earth System Grid Federation. https://doi.org/10.22033/ESGF/CMIP6.3503

Shiogama H, Abe M, Tatebe H (2019a) MIROC MIROC6 model output prepared for CMIP6 ScenarioMIP ssp126. Version 20190627. Earth System Grid Federation. http://doi.org/10.22033/ESGF/CMIP6.5743

Shiogama H, Abe M, Tatebe H (2019b) MIROC MIROC6 model output prepared for CMIP6 ScenarioMIP ssp585. Version 20190627. Earth System Grid Federation. http://doi.org/10.22033/ESGF/CMIP6.5771

Swart NC, Cole JNS, Kharin V V., Lazare M, Scinocca JF, Gillett NP, Anstey J, Arora V, Christian JR, Jiao Y, Lee WG, Majaess F, Saenko OA, Seiler C, Seinen C, Shao A, Solheim L, von Salzen K, Yang D, Winter B, Sigmond M (2019a) CCCma CanESM5 model output prepared for CMIP6 ScenarioMIP ssp585.

Version 20190429. Earth System Grid Federation. http://doi.org/10.22033/ESGF/CMIP6.3696

Swart NC, Cole JNS, Kharin V V, Lazare M, Scinocca JF, Gillett NP, Anstey J, Arora V, Christian JR, Jiao Y, Lee WG, Majaess F, Saenko OA, Seiler C, Seinen C, Shao A, Solheim L, von Salzen K, Yang D, Winter B, Sigmond M (2019b) CCCma CanESM5 model output prepared for CMIP6 CMIP historical. Version 20190429. Earth System Grid Federation. http://doi.org/10.22033/ESGF/CMIP6.3696

Swart NC, Cole JNS, Kharin V V, Lazare M, Scinocca JF, Gillett NP, Anstey J, Arora V, Christian JR, Jiao Y, Lee WG, Majaess F, Saenko OA, Seiler C, Seinen C, Shao A, Solheim L, von Salzen K, Yang D, Winter B, Sigmond M (2019c) CCCma CanESM5 model output prepared for CMIP6 ScenarioMIP ssp126. Version 20190429. Earth System Grid Federation. http://doi.org/10.22033/ESGF/CMIP6.3683

Tatebe H, Watanabe M (2018) MIROC MIROC6 model output prepared for CMIP6 CMIP historical. Version 20181212. Earth System Grid Federation. http://doi.org/10.22033/ESGF/CMIP6.5603

Wu T, Chu M, Dong M, Fang Y, Jie W, Li J, Li W, Liu Q, Shi X, Xin X, Yan J, Zhang F, Zhang J, Zhang L, Zhang Y (2018) BCC BCC-CSM2MR model output prepared for CMIP6 CMIP historical. Version 20181126. Earth System Grid Federation. http://doi.org/10.22033/ESGF/CMIP6.2948

Xin X, Wu T, Shi X, Zhang F, Li J, Chu M, Liu Q, Yan J, Ma Q, Wei M (2019a) BCC BCC-CSM2MR model output prepared for CMIP6 ScenarioMIP ssp126. Verison 20190314. Earth System Grid Federation. http://doi.org/10.22033/ESGF/CMIP6.3028

Xin X, Wu T, Shi X, Zhang F, Li J, Chu M, Liu Q, Yan J, Ma Q, Wei M (2019b) BCC BCC-CSM2MR model output prepared for CMIP6 ScenarioMIP ssp585. Version 20190314. Earth System Grid Federation. http://doi.org/10.22033/ESGF/CMIP6.3050

Yukimoto S, Koshiro T, Kawai H, Oshima N, Yoshida K, Urakawa S, Tsujino H, Deushi M, Tanaka T, Hosaka M, Yoshimura H, Shindo E, Mizuta R, Ishii M, Obata A, Adachi Y (2019a) MRI MRI-ESM2.0 model output prepared for CMIP6 CMIP historical. Version 20190222. Earth System Grid Federation. http://doi.org/10.22033/ESGF/CMIP6.6842

Yukimoto S, Koshiro T, Kawai H, Oshima N, Yoshida K, Urakawa S, Tsujino H, Deushi M, Tanaka T, Hosaka M, Yoshimura H, Shindo E, Mizuta R, Ishii M, Obata A, Adachi Y (2019b) MRI MRI-ESM2.0 model output prepared for CMIP6 ScenarioMIP ssp126. Version 20191108. Earth System Grid Federation. http://doi.org/10.22033/ESGF/CMIP6.6909

Yukimoto S, Koshiro T, Kawai H, Oshima N, Yoshida K, Urakawa S, Tsujino H, Deushi M, Tanaka T, Hosaka M, Yoshimura H, Shindo E, Mizuta R, Ishii M, Obata A, Adachi Y (2019c) MRI MRI-ESM2.0 model output prepared for CMIP6 ScenarioMIP ssp585. Version 20191108. Earth System Grid Federation. http://doi.org/10.22033/ESGF/CMIP6.6929

Supplemental Table A2.2: Correlation parameters between yearly averaged observed air temperature from TF Green station and sea surface temperature at the URI GSO fish trawl Fox Island station for 1960-2018. The slope was highly significant.

| Coefficient | Estimate | Standard Error | P-value |
|---|---|---|---|
| Intercept | 1.7190 | 1.3651 | 0.2 |
| Slope | 0.9242 | 0.1281 | <0.001 *** |

*Supplement 3: Thermal response parameters*

Parameters needed to create the Kitchell curves were chosen through a standardized methodology, which differed by parameter. This protocol ensured that the parameters chosen best represented the fish in the model, and that the parameters were as comparable to each other as possible. Literature was searched with GoogleScholar, and search terms included a combination of the common and scientific name with one or more of the following terms: temperature, consumption, metabolism, respiration, $Q_{10}$, thermal, tolerance, $Ct_{max}$. Adults were distinguished from juvenile life stages by how the author described their samples in the study. Fish referred to as 'adults' were considered adults. Fishbase (Froese and Pauly, 2019) length at first maturity was used to make a determination in absence of other data.

Maximum temperature

The maximum temperature was rounded to a whole degree using the ceiling function to ensure the rounded maximum temperature encompassed the reported temperature.

Three main data sources were considered, and the highest value for each species were chosen as the final maximum temperature. The three data sources were 1) the temperature recorded during the GSO fish trawl for tows in which the species was caught, 2) the website Aquamaps, which gathers temperature of occurrence data from multiple established surveys (Kaschner et al. 2019), and 3) values from experimental literature in which temperature tolerances for adults of the species were examined. Thermal data from Essential Fish Habitat (EFH) reports for species were found to already be accounted for by the Aquamaps site or experimental studies, so EFH documents were not considered one of the main three data sources. Studies from

geographically dissimilar stocks (i.e. Gulf of Mexico) were not included, as the temperatures of those individuals may not be representative of the fishes coming to Narragansett Bay.

Supplemental Table A3.1: Source data for the species thermal maximum $T_{max}$ (°C) parameter.

| Species | $T_{max}$ value | Source |
|---|---|---|
| Atlantic menhaden | 30 | Wyllie et al. (1976) |
| Atlantic moonfish | 33 | Aquamaps |
| Alewife | 33 | Otto et al. (1976) |
| Bay anchovy | 33 | Luo & Brandt (1993) |
| Atlantic silverside | 31 | Hoff & Westman (1966) |
| Atlantic herring | 26 | Aquamaps |
| Butterfish | 27 | GSO |
| Blueback herring | 27 | Aquamaps |
| Winter flounder | 26 | GSO |
| Tautog | 29 | Olla et al. (1978) |
| Scup | 30 | Aquamaps |
| Black sea bass | 30 | Slesinger et al. (2019) |
| Little skate | 26 | Aquamaps |
| Striped searobin | 27 | GSO |
| Summer flounder | 28 | Aquamaps |
| Atlantic striped bass | 28 | Nelson et al. (2010) |
| Bluefish | 32 | Aquamaps |
| Weakfish | 27 | Aquamaps |
| Spiny dogfish | 29 | Aquamaps |

Temperature of maximum consumption

The temperature of maximum consumption was rounded to the nearest whole degree. We created a hierarchy of options and the value of the parameter from the highest ranked source was chosen. If there were two studies at the same level, such as two experimental studies on adults, then the average of the values was taken. In order from highest to lowest:

1. Study for adults describing the temperature of maximum consumption; if a range was given due to acclimation temperatures, the average was taken.
2. A temperature of maximum consumption in a published adult model.
3. Study for subadults (juveniles or post-larval stages) describing temperature of maximum consumption.
4. A temperature of maximum consumption in a published subadult model.
5. The average of a published temperature of optimum growth and the maximum temperature, as theory states that the temperature of maximum consumption is greater than the temperature of optimum growth ($T_{optGrowth}$; Jobling, 1994).
6. In the absence of other data, the temperature of maximum consumption is assumed to be 90% of the maximum temperature. This is based on the typical shape of the Kitchell curve as it is described as a skewed curve with a steep drop off. That shape can only be achieved with a temperature of maximum consumption near the maximum temperature.

Supplemental Table A3.2: Source data for the species temperature of maximum consumption $T_{optC}$ (°C) parameter.

| Species | Decision Category | Parameter Estimate | Source |
|---|---|---|---|
| Atlantic menhaden | Subadult Experiment | 28 | Rippetoe (1993) |
| Atlantic moonfish | Assumed 90% $T_{max}$ | 30 | |
| Alewife | Adult Model | 17 | Stewart & Binkowski (1986) |
| Bay anchovy | Adult Model | 28 | Luo & Brandt (1993), Rose et al. (1999) |
| Atlantic silverside | Average of $T_{optGrowth}$ & $T_{max}$ | 28 | Murray & Baumann (2018) |
| Atlantic herring | Adult model | 16 | Rudstam (1988) |
| Butterfish | Assumed 90% $T_{max}$ | 24 | |
| Blueback herring | Assumed 90% $T_{max}$ | 25 | |
| Winter flounder | Subadult Model | 16 | Rose et al. (1996) |
| Tautog | Adult Experiment | 28 | Olla et al. (1978) |
| Scup | Assumed 90% $T_{max}$ | 27 | |
| Black sea bass | Average of $T_{optGrowth}$ & $T_{max}$ | 26 | Berlinsky et al. (2000) |
| Little skate | Assumed 90% $T_{max}$ | 23 | |
| Striped searobin | Assumed 90% $T_{max}$ | 24 | |
| Summer flounder | Average of $T_{optGrowth}$ & $T_{max}$ | 23 | Malloy & Targett (1991) |
| Atlantic striped bass | Subadult Experiment | 23 | Hartman & Brandt (1995) |
| Bluefish | Subadult Experiment | 28 | Buckel et al. (1995); Hartman and Brandt (1995) |
| Weakfish | Subadult Experiment | 26 | Lankford Jr & Targett (1994), Hartman & Brandt (1995) |
| Spiny dogfish | Subadult Model | 19 | Harvey (2009) |

$Q_{10}$ consumption

The $Q_{10}$ value for consumption is rounded to one decimal place. We created a hierarchy of options and the value of the parameter from the highest ranked source was chosen. If there were two studies at the same level, such as two experimental studies on adults, then the average of the values was taken. If multiple $Q_{10}$ values were reported, such as for different individuals or temperature ranges, the average was taken. The $Q_{10}$ could be calculated using Eq. (A3.1), where $V_1$ and $V_2$ are the consumption rates measured at temperatures the $T_1$ and $T_2$, respectively.

$$\mathbf{Q_{10}} = (\mathbf{V_1}/\mathbf{V_2})^{\frac{\mathbf{10}}{[\mathbf{T2}-\mathbf{T1}]}} \qquad (\boldsymbol{A3.1})$$

In order from highest to lowest:

1. A $Q_{10}$ reported by a consumption study for adults.
2. A $Q_{10}$ from a published adult bioenergetics model.
3. A $Q_{10}$ calculated from a temperature-dependent consumption study on adults. Note: If calculating from the Thorton & Lessem method of bioenergetic models, the KA value was calculated with the K1 and K2 and θ1 and θ2. The environmental T1 was chosen as θ1 + 2°C and θ2 + 2°C for T2. The $Q_{10}$ was calculated from the KA values.
4. A $Q_{10}$ reported by a consumption study for subadults.
5. A $Q_{10}$ from a published subadult bioenergetics model.
6. A $Q_{10}$ calculated from a temperature-dependent consumption study on subadults. Note: Calculated method will be the same as used for adults.
7. In the absence of other data, a default of 2.3, which is the recommended default in the Fish Bioenergetics software (Hansen et al., 1997).

Supplemental Table A3.3: Source data for the species $Q_{10}$ of consumption parameter.

| Species | Decision Category | Parameter Estimate | Source |
|---|---|---|---|
| Atlantic menhaden | Subadult Model | 2.1 | Rippetoe (1993) |
| Atlantic moonfish | Default | 2.3 | |
| Alewife | Adult Calculated | 2.4 | Stewart & Binkowski (1986) |
| Bay anchovy | Adult Model | 2.2 | Luo & Brandt (1993) |
| Atlantic silverside | Adult Calculated | 2.0 | Billerbeck et al. (2000) |
| Atlantic herring | Adult Calculated | 2.3 | Rudstam (1988) |
| Butterfish | Default | 2.3 | |
| Blueback herring | Default | 2.3 | |
| Winter flounder | Adult Calculated | 1.8 | Worobec (1984) |
| Tautog | Default | 2.3 | |
| Scup | Default | 2.3 | |
| Black sea bass | Default | 2.3 | |
| Little skate | Default | 2.3 | |
| Striped searobin | Default | 2.3 | |
| Summer flounder | Subadult Calculated | 3.1* | Malloy & Targett (1991) |
| Atlantic striped bass | Adult Model | 2.3 | Brandt (1993) |
| Bluefish | Subadult Model | 2.6 | Hartman & Brandt (1995) |
| Weakfish | Subadult Model | 2.9 | Hartman & Brandt (1995) |
| Spiny dogfish | Subadult Model | 2.5 | Harvey (2009) |

*Subadult study from Malloy & Targett gave an average $Q_{10}$ of 7.1, well above what is recorded for other species. The consumption curve created with that high $Q_{10}$ did not match the shape as specified in bioenergetic theory. The $Q_{10}$ value was lowered by choosing only the estimates of feeding from 6°C to 10°C.

Species-specific biomass time series were used to create a weighted average of the thermal response curves by functional groups (Supplemental Table A3.4). The time series were the same as those used in Innes-Gold et al (2020).

Supplemental Table A3.4: 1994-1998 averages of species-specific biomasses were used to weight the thermal parameters. Data were taken from the GSO and DEM trawls, with more detail found in Innes-Gold et al. (2020). Biomasses in $g/m^2$ have been rounded to four decimal points.

| Species | 1994-1998 Averaged Biomass Category |
|---|---|
| Atlantic menhaden | 0.7334 |
| Atlantic moonfish | 0.0189 |
| Alewife | 0.1753 |
| Bay anchovy | 1.2785 |
| Atlantic silverside | 0.7437 |
| Atlantic herring | 7.3930 |
| Butterfish | 0.9619 |
| Blueback herring | 0.1942 |
| Winter flounder | 0.8141 |
| Tautog | 0.0966 |
| Scup | 0.5536 |
| Black sea bass | 0.0110 |
| Little skate | 6.0877 |
| Striped searobin | 0.1245 |
| Summer flounder | 0.5532 |
| Atlantic striped bass | 0.0241 |
| Bluefish | 0.1232 |
| Weakfish | 0.0977 |
| Spiny dogfish | 0.2424 |

*Supplement 4: Sensitivity tests*

Supplemental Table A4.1: Southern species used to assess sensitivity of the consumption curve to changing community composition. Species were chosen as those that have been caught in Narragansett Bay in the last 15 years according to the GSO trawl data and are currently found in the Chesapeake Bay (Buchheister et al., 2013; Jung and Houde, 2003). Functional group was assigned after consulting the diet as reported in Bowman et al. (2000). All have warmer thermal maxima than the species of the original model. Maximum temperature was taken as the extreme value of the temperature of catch from the GSO fish trawl and the website Aquamaps (accessed March 2021). The temperature of optimum consumption was assumed to be 90% of the maximum temperature, and $Q_{10}$ was assumed to be 2.3. The biomass values were chosen as the median biomass of the original species that made up the functional group, so the species was represented similarly the others of the functional group.

| Species | Scientific Name | Functional Group | $T_{max}$ | $T_{optC}$ | Biomass ($g/m^2$) |
|---|---|---|---|---|---|
| Spot | *Leiostomus xanthurus* | Benthivorous Fish | 31 | 27.9 | 0.3390 |
| Spotted Hake | *Urophycis regia* | Piscivorous Fish | 30 | 27.0 | 0.1232 |
| Striped Anchovy | *Anchoa hepsetus* | Planktivorous Fish | 33 | 29.7 | 0.7384 |
| Harvestfish | *Peprilus paru* | Planktivorous Fish | 33 | 29.7 | 0.7384 |
| Inshore Lizardfish | *Synodus foetens* | Piscivorous Fish | 33 | 29.7 | 0.1232 |
| Gulf Stream Flounder | *Citharichthyes arctifrons* | Benthivorous Fish | 31 | 27.9 | 0.3390 |
| Clearnose Skate | *Raja eglanteria* | Piscivorous Fish | 30 | 27.0 | 0.1232 |
| Smooth Dogfish | *Mustelus canis* | Benthivorous Fish | 33 | 29.7 | 0.3390 |
| Northern Kingfish | *Menticirrhus saxatilis* | Benthivorous Fish | 31 | 27.9 | 0.3390 |

The second sensitivity test examines scaling by different temperatures. For this test, $T_{QB}$, or the temperature that informed the Ecopath *Q/B* parameter, was the species-specific biomass weighted average of the individual temperature that informed each species' original *Q/B* input. The relative consumption was scaled according to Eq. (3), except the Kitchell modifier was evaluated at the $T_{QB}$ of each functional group instead of $T_{B94}$. The respiration thermal response was scaled similarly to what was

done for the consumption response, so that a modifier of 1.0 on the scaled respiration curve (i.e. Blanchard curve) was associated with the temperature that informed the Ecopath *P/B* parameter ($T_{PB}$). In EwE, the *P/B* parameter is estimated as total mortality (*Z*) which is the sum of natural mortality (*M*) and fishing mortality (*F*) (Christensen et al., 2008). The natural mortality input literature generally reported temperatures, and the temperature of fishing mortality was assumed to be the 1994-1998 yearly averaged temperature of Narragansett Bay as the *F* values were calculating from Bay catches. In cases for which temperature of natural mortality was not reported, it was assumed to be the average of the 5$^{th}$ and 95$^{th}$ percentiles for temperature reported in Aquamaps (Kaschner et al., 2019). The temperature of natural mortality ($T_M$) and fishing mortalities ($T_F$) were averaged to determine $T_{PB}$. The relative respiration was calculated according to Eq. (5) except that the original Blanchard modifier was evaluated at the mean of $T_M$ and $T_F$ instead of $T_{B94}$.

The temperature of Ecopath ($T_{Eco}$) for each functional group was considered to be the average $T_{QB}$ and $T_{PB}$, described earlier. Total respiration was set so that, at $T_{Eco}$, total consumption divided by total respiration was equal to the original ActiveRespFrac of the base model version. Total respiration was calculated according to Eq. (7) except that the total consumption and relative biomass curves were evaluated at $T_{Eco}$ instead of $T_{B94}$. All temperatures by functional group are listed in Supplemental Table A4.2.

Supplemental Table A4.2. Temperatures by functional group used in the second sensitivity test. Note that $T_F$ is calculated the same as $T_{B94}$.

| Functional Group | $T_{QB}$ | $T_M$ | $T_F$ | $T_{PB}$ | $T_{Eco}$ | $T_{B94}$ |
|---|---|---|---|---|---|---|
| Benthivorous Fish | 14.53 | 14.92 | 11.7 | 13.12 | 13.8 | 11.7 |
| Planktivorous Fish | 13.19 | 12.13 | 11.7 | 11.94 | 12.6 | 11.7 |
| Piscivorous Fish | 19.32 | 18.75 | 11.7 | 15.25 | 17.3 | 11.7 |

*References for Appendix A*

Berlinsky, D., Watson, M., Nardi, G., Bradley, T.M., 2000. Investigations of selected parameters for growth of larval and juvenile black sea bass *Centropristis striata* L. J. World Aquac. Soc. 31, 426–435. https://doi.org/10.1111/j.1749-7345.2000.tb00892.x

Billerbeck, J.M., Schultz, E.T., Conover, D.O., 2000. Adaptive variation in energy acquisition and allocation among latitudinal populations of the Atlantic silverside. Oecologia 122, 210–219. https://doi.org/10.1007/PL00008848

Bowman, R.E., Stillwell, C.E., Michaels, W.L., Grosslein, M.D., 2000. Food of northwest Atlantic fishes and two common species of squid. U.S. Dep. Commer. NOAA Tech. Memo. NMFS-NE 155. https://doi.org/10.5962/bhl.title.4024

Brandt, S.B., 1993. The effect of thermal fronts on fish growth: A bioenergetics evaluation of food and temperature. Estuaries 16, 142–159.

Buchheister, A., Bonzek, C.F., Gartland, J., Latour, R.J., 2013. Patterns and drivers of the demersal fish community of Chesapeake Bay. Mar. Ecol. Prog. Ser. 481, 161–180. https://doi.org/doi: 10.3354/meps10253

Buckel, J. A., Steinberg, N.D., Conover, D.O., 1995. Effects of temperature, salinity, and fish size on growth and consumption of juvenile bluefish. J. Fish Biol. 47, 696–706. https://doi.org/https://doi.org/10.1111/j.1095-8649.1995.tb01935.x

Christensen, V., Walters, C.J., Pauly, D., Forrest, R., 2008. Ecopath with Ecosim version 6 User Guide.

Hansen, P., Johnson, T., Schindler, D.E., Kitchell, J., 1997. Fish Bioenergetics 3.0 Manual. Fish Bioenerg. 3.0.

Hartman, K.J., Brandt, S.B., 1995. Comparative energetics and the development of bioenergetics models for sympatric estuarine piscivores. Can. J. Fish. Aquat. Sci. 52, 1647–1666. https://doi.org/10.1139/f95-759

Harvey, C.J., 2009. Effects of temperature change on demersal fishes in the California Current: A bioenergetics approach. Can. J. Fish. Aquat. Sci. 66, 1449–1461. https://doi.org/10.1139/F09-087

Hoff, J.G., Westman, J.R., 1966. The temperature tolerances of three species of marine fishes. J. Mar. Res.

Innes-Gold, A., Heinichen, M., Gorospe, K., Truesdale, C., Collie, J., Humphries, A., 2020. Modeling 25 years of food web changes in Narragansett Bay (USA) as a tool for ecosystem-based management. Mar. Ecol. Prog. Ser. 654, 17–33. https://doi.org/10.3354/meps13505

Jobling, M., 1994. Fish Bioenergetics, First edit. ed. Chapman & Hall.

Jung, S., Houde, E.D., 2003. Spatial and temporal variabilities of pelagic fish community structure and distribution in Chesapeake Bay, USA. Estuar. Coast. Shelf Sci. 58, 335–351. https://doi.org/10.1016/S0272-7714(03)00085-4

Kaschner, K., Kesner-Reyes, K., Garilao, C., Rius-Barile, J., Rees, T., Froese, R., 2019. Aquamaps: Predicted range maps for aquatic species. www.aquamaps.org. Accessed October 2020

Lankford Jr, T., Targett, T., 1994. Suitability of estuarine nursery zones for juvenile weakfish (*Cynoscion regalis*): effects of temperature and salinty on feeding, growth and survival. Mar. Biol. 119, 611–620.

Luo, J., Brandt, S.B., 1993. Bay anchovy *Anchoa mitchilli* production and consumption in mid- Chesapeake Bay based on a bioenergetics model and acoustic measures of fish abundance. Mar. Ecol. Prog. Ser. 98, 223–236. https://doi.org/10.3354/meps098223

Malloy, K.D., Targett, T.E., 1991. Feeding, growth and survival of juvenile summer flounder *Paralichthys dentatus*: experimental analysis of the effects of temperature and salinity. Mar. Ecol. Prog. Ser. 72, 213–223.

Murray, C.S., Baumann, H., 2018. You Better Repeat It: Complex CO 2 × Temperature Effects in Atlantic Silverside Offspring Revealed by Serial Experimentation. Diversity 10, 69. https://doi.org/https://doi.org/10.3390/d10030069

Nelson, G.A., Armstrong, M.P., Stritzel-Thomson, J., Friedland, K.D., 2010. Thermal habitat of striped bass (*Morone saxatilis*) in coastal waters of northern Massachusetts, USA, during summer. Fish. Oceanogr. 19, 370–381. https://doi.org/10.1111/j.1365-2419.2010.00551.x

Olla, B.L., Studholme, A.L., Bejda, A.J., Samet, C., Martin, A.D., 1978. Effect of temperature on activity and social behavior of the adult tautog *Tautoga onitis* under laboratory conditions. Mar. Biol. 45, 369–378. https://doi.org/10.1007/BF00391823

Otto, R.G., Kitchel, M.A., Rice, J.O., 1976. Lethal and Preferred Temperatures of the Alewife (*Alosa pseudoharengus*) in Lake Michigan. Trans. Am. Fish. Soc. 105, 96–106. https://doi.org/10.1577/1548-8659(1976)105<96:laptot>2.0.co;2

Rippetoe, T., 1993. Production and energetics of Atlantic menhaden in Chesapeake Bay. University of Maryland.

Rose, K.A., Tyler, J.A., Chambers, R.C., Klein-MacPhee, G., Danila, D.J., 1996. Simulating winter flounder population dynamics using coupled individual-based young-of-the-year and age-structured adult models. Can. J. Fish. Aquat. Sci. 53, 1071–1091. https://doi.org/10.1139/cjfas-53-5-1071

Rose, K.A., Cowan, J.H., Clark, M.E., Houde, E.D., Wang, S. Bin, 1999. An individual-based model of bay anchovy population dynamics in the mesohaline region of Chesapeake Bay. Mar. Ecol. Prog. Ser. 185, 113–132. https://doi.org/10.3354/meps185113

Rudstam, L.G., 1988. Exploring the dynamics of herring consumption in the Baltic: Applications of an energetic model of fish growth. Kieler Meeresforsch. Sonderh. 6, 312–322.

Slesinger, E., Andres, A., Young, R., Seibel, B., Saba, V., Phelan, B., Rosendale, J., Wieczorek, D., Saba, G., 2019. The effect of ocean warming on black sea bass (*Centropristis striata*) aerobic scope and hypoxia tolerance. PLoS One 14, e0218390. https://doi.org/10.1371/journal.pone.0218390

Stewart, D.J., Binkowski, F.P., 1986. Dynamics of Consumption and Food Conversion by Lake Michigan Alewives: An Energetics-Modeling Synthesi. Trans. Am. Fish. Soc. 115, 643–661.

Worobec, M.N., 1984. Field estimates of the daily ration of winter flounder, *Pseudopleuronectes americanus* (Walbaum), in a southern New England salt pond. J. Exp. Biol. 77, 183–196. https://doi.org/https://doi.org/10.1016/0022-0981(84)90057-1

Wyllie, M.C., Holmstrom, E.R., Wallace, R.K., 1976. Temperature preference, avoidance, shock, and swim speed studies with marine and estuarine organisms from New Jersey. Newark, NJ.

## Appendix B: Supplementary Results

*Supplement 1: Temperature*

Table B1.1: Surface water temperature (°C) time series used to force the temperature-dependent versions of the model. Temperatures from 1994-2018 were observed from Narragansett Bay. High and low warming scenario temperatures for 2019-2054 were projected using the CMIP6 models.

| Year | Observed Temp. | Low Warming SSP1-2.6 | High Warming SSP5-8.5 | Year | Low Warming SSP1-2.6 | High Warming SSP5-8.5 |
|---|---|---|---|---|---|---|
| 1994 | 11.8 | | | 2025 | 12.7 | 12.9 |
| 1995 | 12 | | | 2026 | 12.8 | 12.9 |
| 1996 | 11 | | | 2027 | 13.3 | 12.9 |
| 1997 | 11.6 | | | 2028 | 13.2 | 12.6 |
| 1998 | 12.4 | | | 2029 | 12.9 | 12.8 |
| 1999 | 12.7 | | | 2030 | 13.4 | 12.8 |
| 2000 | 11.6 | | | 2031 | 13.4 | 12.7 |
| 2001 | 12 | | | 2032 | 13.2 | 13.2 |
| 2002 | 12.1 | | | 2033 | 13.5 | 13.1 |
| 2003 | 11.2 | | | 2034 | 13.1 | 13.1 |
| 2004 | 11.4 | | | 2035 | 13.5 | 13.4 |
| 2005 | 11.8 | | | 2036 | 13.1 | 13.2 |
| 2006 | 12.7 | | | 2037 | 13.1 | 13.6 |
| 2007 | 11.9 | | | 2038 | 13.5 | 13.6 |
| 2008 | 12.1 | | | 2039 | 13.4 | 13.5 |
| 2009 | 11.6 | | | 2040 | 13.6 | 13.8 |
| 2010 | 11.6 | | | 2041 | 13.5 | 13.5 |
| 2011 | 12.4 | | | 2042 | 13.1 | 13.5 |
| 2012 | 13.8 | | | 2043 | 13.5 | 13.8 |
| 2013 | 12.2 | | | 2044 | 13.1 | 13.7 |
| 2014 | 11.8 | | | 2045 | 13.1 | 14.2 |
| 2015 | 12 | | | 2046 | 13.2 | 14.2 |
| 2016 | 12.7 | | | 2047 | 13.2 | 14.1 |
| 2017 | 12.2 | | | 2048 | 13.8 | 14.2 |
| 2018 | 12.4 | | | 2049 | 13.4 | 14.3 |
| 2019 | | 13.1 | 12.6 | 2050 | 13.7 | 14.3 |
| 2020 | | 12.8 | 12.7 | 2051 | 13.7 | 14.2 |
| 2021 | | 13 | 12.6 | 2052 | 13.2 | 14.1 |
| 2022 | | 12.9 | 13 | 2053 | 13.7 | 14.2 |
| 2023 | | 12.9 | 12.7 | 2054 | 13.7 | 14 |
| 2024 | | 12.7 | 12.6 | | | |

*Supplement 2: Consumption thermal response curves*

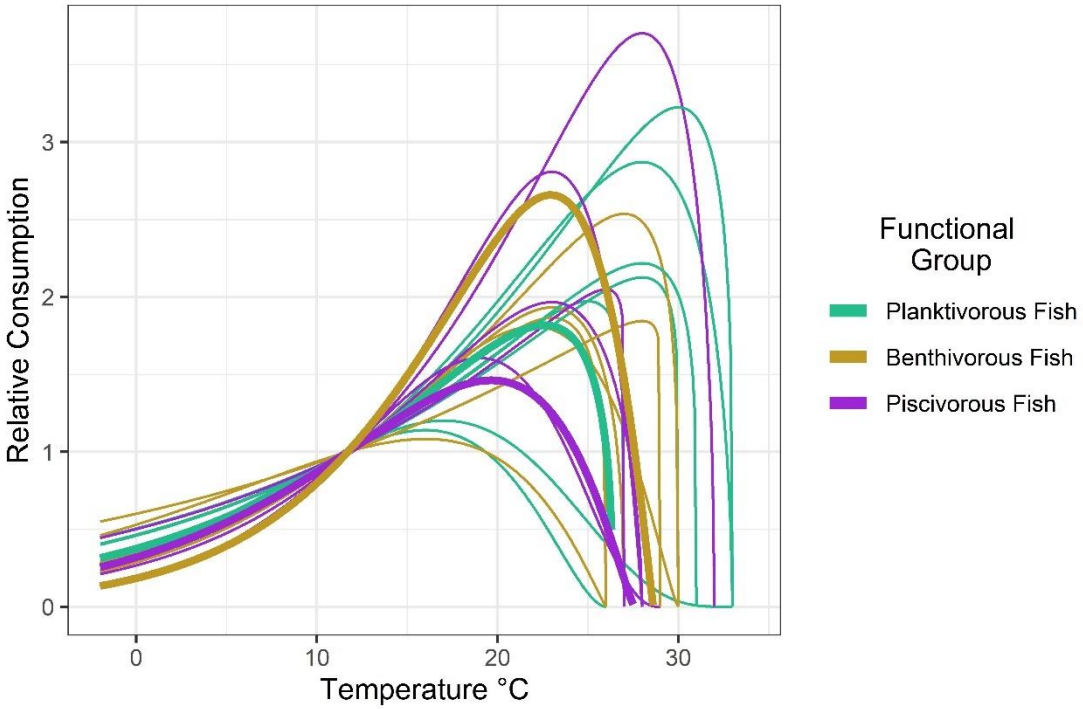


Supplemental Figure B2.1 Relative consumption curves created from the species-specific parameters instead of averaged into a functional group response. Bold lines show the functional group average thermal response.

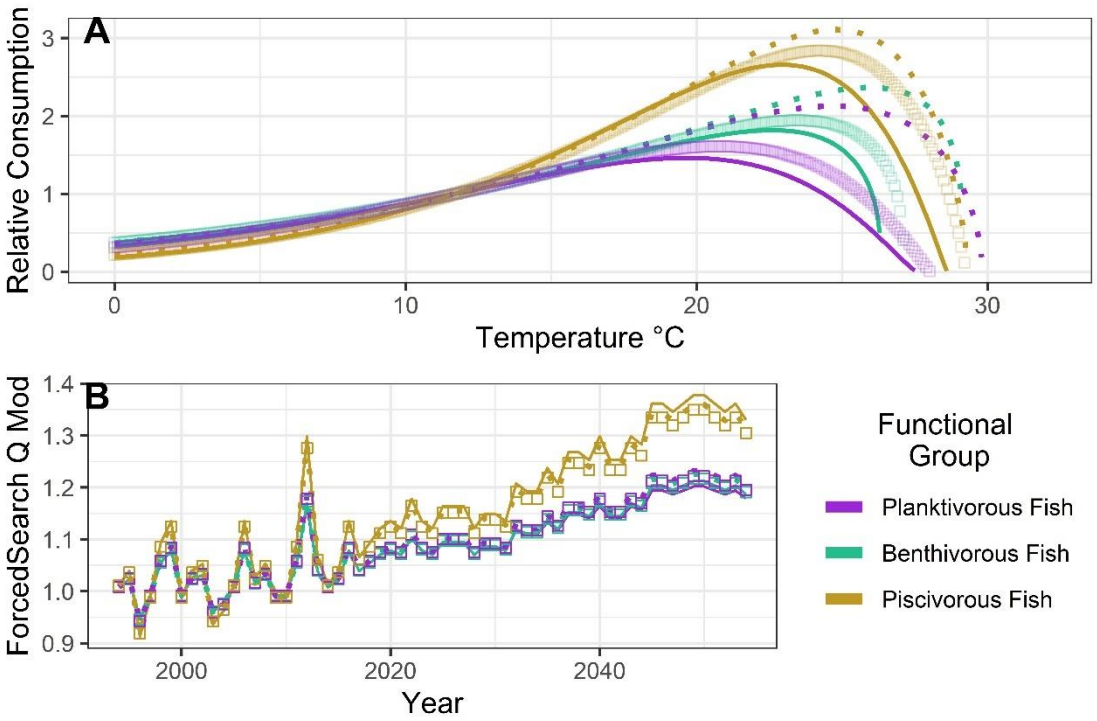


Figure B2.2: A) Relative consumption curves to assess sensitivity of curve to changing species inputs. Solid lines are the consumption curves used in the model versions. The dotted line shows the Kitchell curve for each functional group created using a single year's observed biomasses that resulted in the warmest skewed curve (2018 for benthivorous fish, 2002 for planktivorous fish, 2013 for piscivorous fish). The open squares are the curves created with the additional traditionally southern species to represent a potential future community composition of the fish groups. B) ForcedSearch consumption modifiers from the three curve options for the high warming scenario.

*Supplement 3: Respiration thermal response curves*

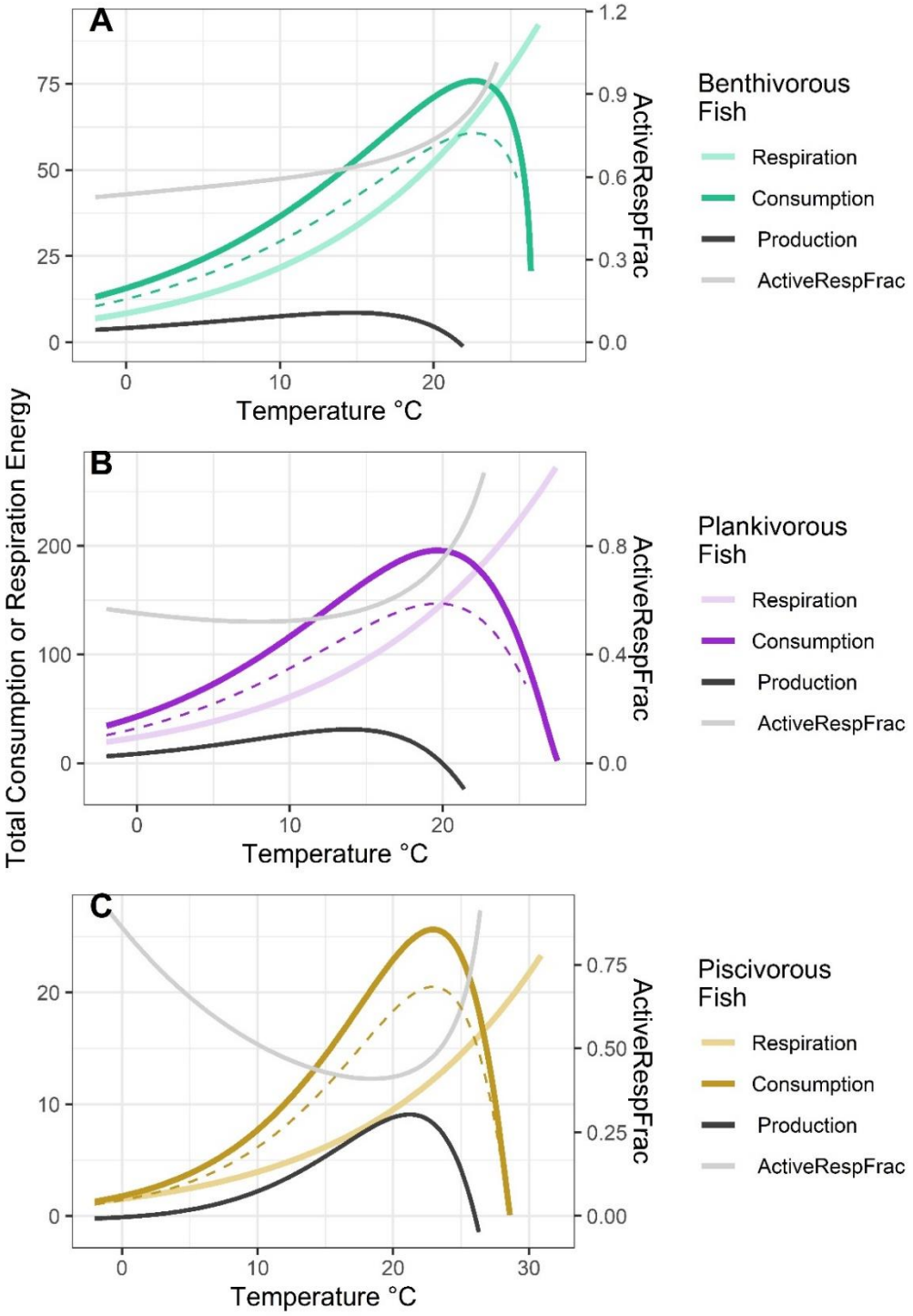


Supplemental Figure B3.1: The total consumption, total respiration, fraction of energy devoted for respiration, and energy available for production for the three fish groups (A-C). The dashed line is the total consumption minus unassimilated food. The grey lines are the ActiveRespFrac curves by temperature as calculated by total respiration divided by total consumption.

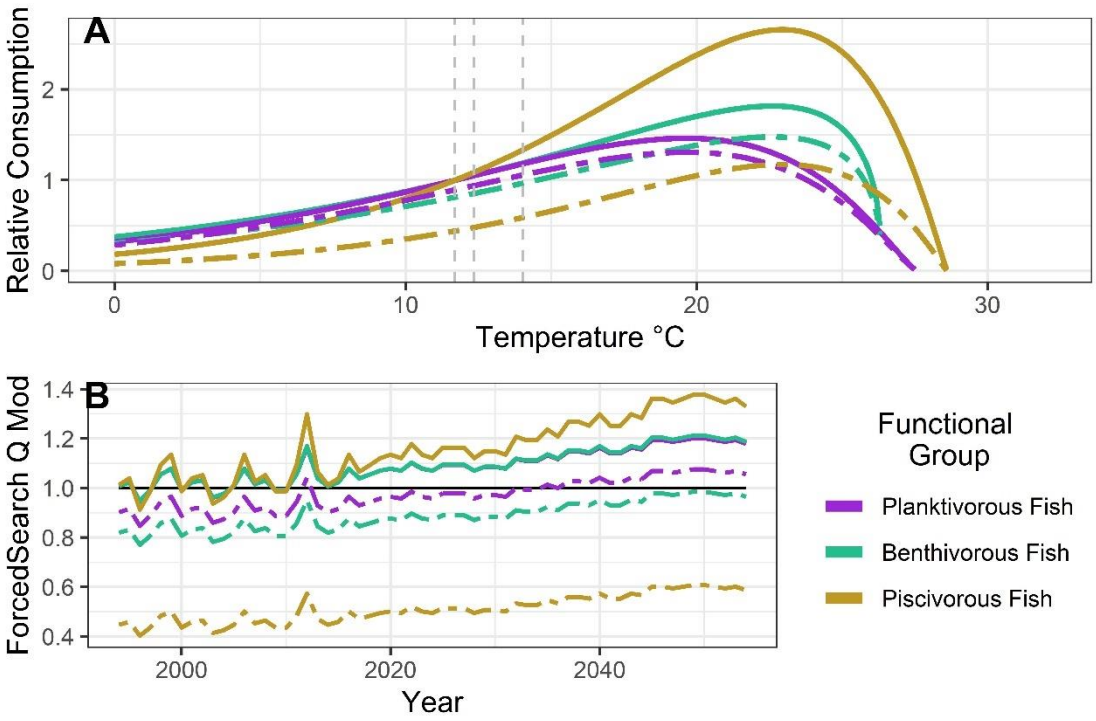


Supplemental Figure B3.2: Relative consumption curve (A) and consumption modifier (B) to assess the sensitivity of the curves to the scaling temperature. Solid lines are the curves and time series used in the model versions. The dashed lines are those scaled to $T_{QB}$. Only the modifiers for the high warming scenario are shown.

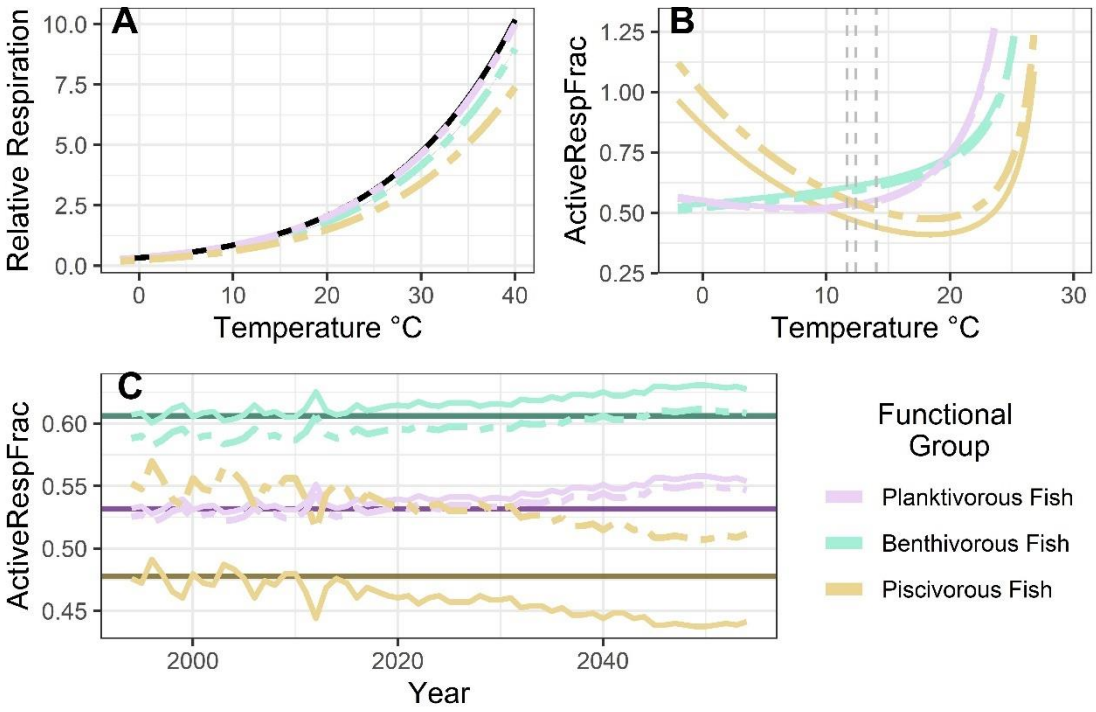


Supplemental Figure B3.3: Relative respiration curve (A), ActiveRespFrac by temperature (B), and respiration modifier (C) to assess the sensitivity of the curves to the scaling temperature. Solid lines are the curves and time series used in the model versions. The dashed lines are those scaled to $T_{PB}$. Only the modifiers for the high warming scenario are shown.

*Supplement 4: Model comparison*

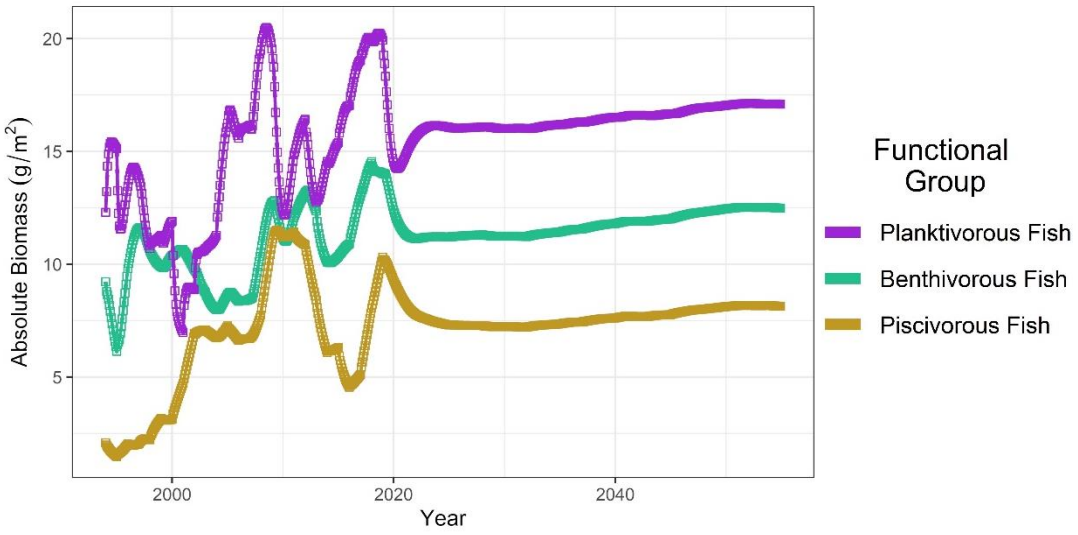


Supplemental Figure B4.1: Fish biomasses run under the different relative consumption curve sensitivity tests. The solid lines are the high warming consumption model version, the dotted lines are the years with the most warm-skewed curve using observed biomasses, and the open squares are the consumption curves made with additional southern species. The differences in biomass were nearly indistinguishable.

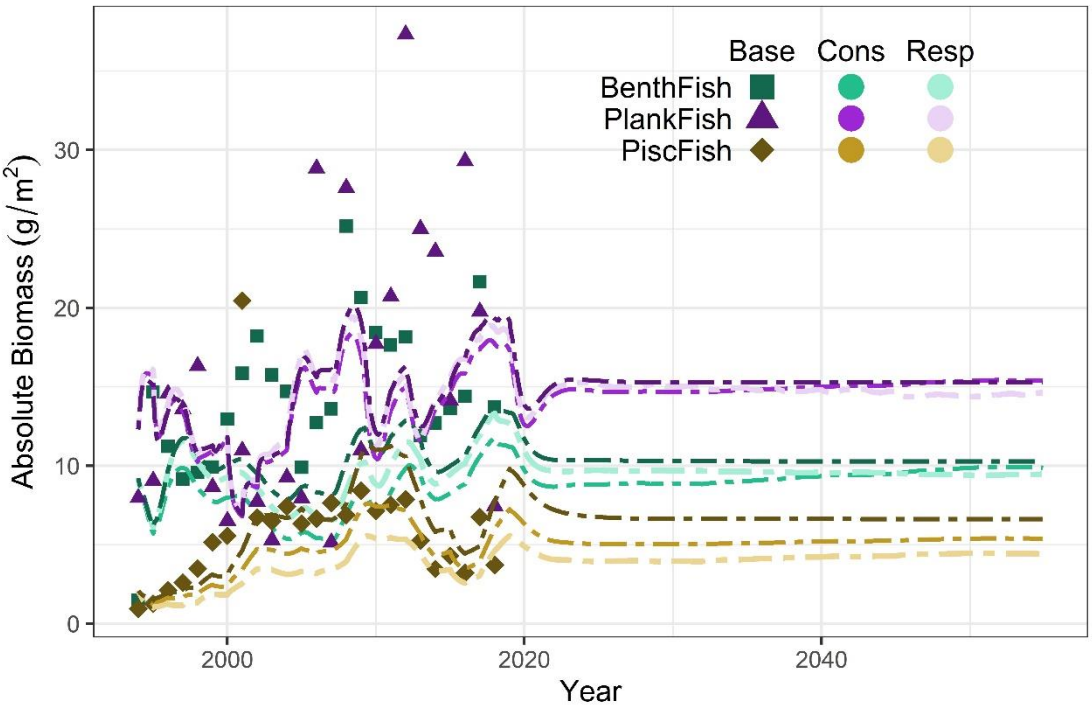


Supplemental Figure B4.2: Fish biomass projections from the second sensitivity test in which relative consumption and respiration curves were scaled to $T_{QB}$ and $T_{PB}$. Color represents the base model and the temperature-dependent models run with the high warming scenario. Points show the input biomass time series of the original Innes-Gold et al. (2020) model.

Supplemental Table B4.1: Absolute biomass sum of squares from 1994-2018 between the observed biomasses and those projected by the different model versions.

| Functional Group | Base | Consumption | Respiration |
|---|---|---|---|
| Piscivorous Fish | 308.5 | 318.8 | 328.0 |
| Benthivorous Fish | 861.5 | 797.6 | 859.9 |
| Planktivorous Fish | 1704.8 | 1696.0 | 1763.0 |
| Carnivorous Benthos | 2858.8 | 2690.2 | 2733.8 |
| Large Squid | 8.6 | 9.2 | 9.1 |
| Small Squid | 15.3 | 15.8 | 15.8 |

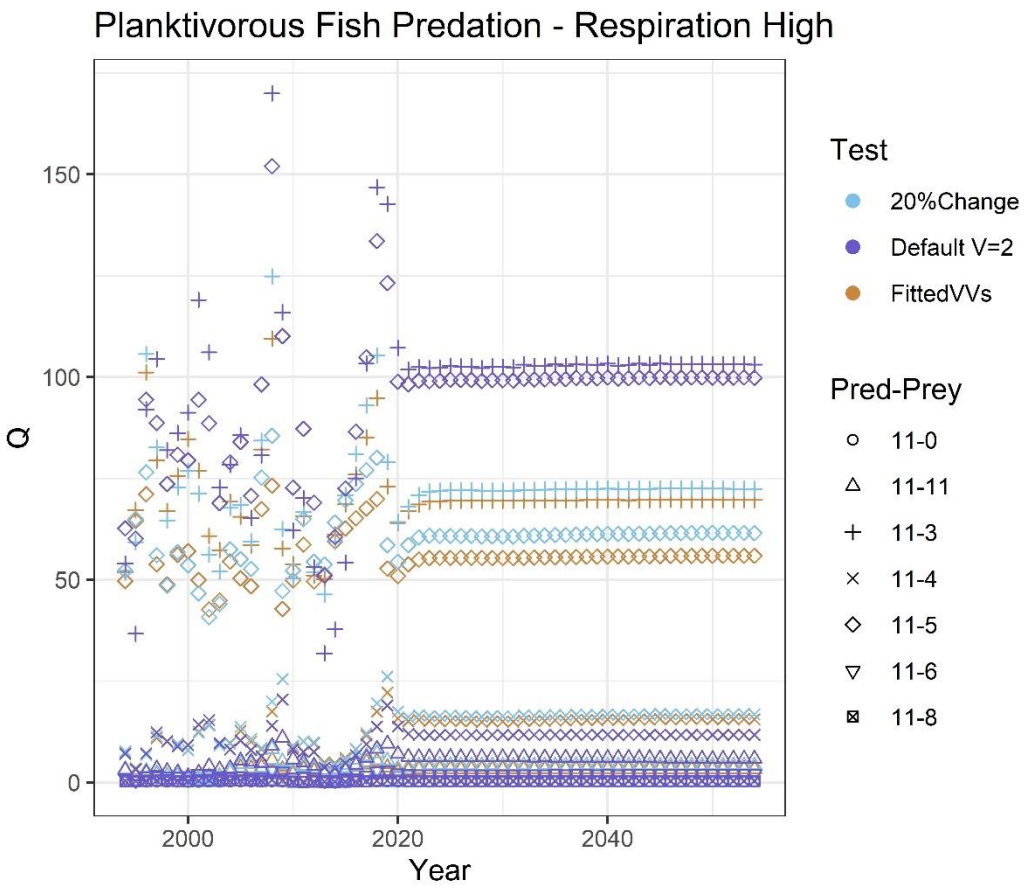


Supplemental Figure B4.3: Rpath Annual Qlink output for the high warming respiration model version testing the impact of different vulnerability values. Q represents consumption, or the energy passing between the predator and prey. The shapes denote different predator prey interactions. The legend gives predator code – prey code. The Rpath functional group codes are given in Supplemental Table A1.1. Only interactions where planktivorous fish are the predator are shown. Fitted vulnerabilities for the strong interactions were 1.01 for 11-3 and 1.0473 for 11-5.

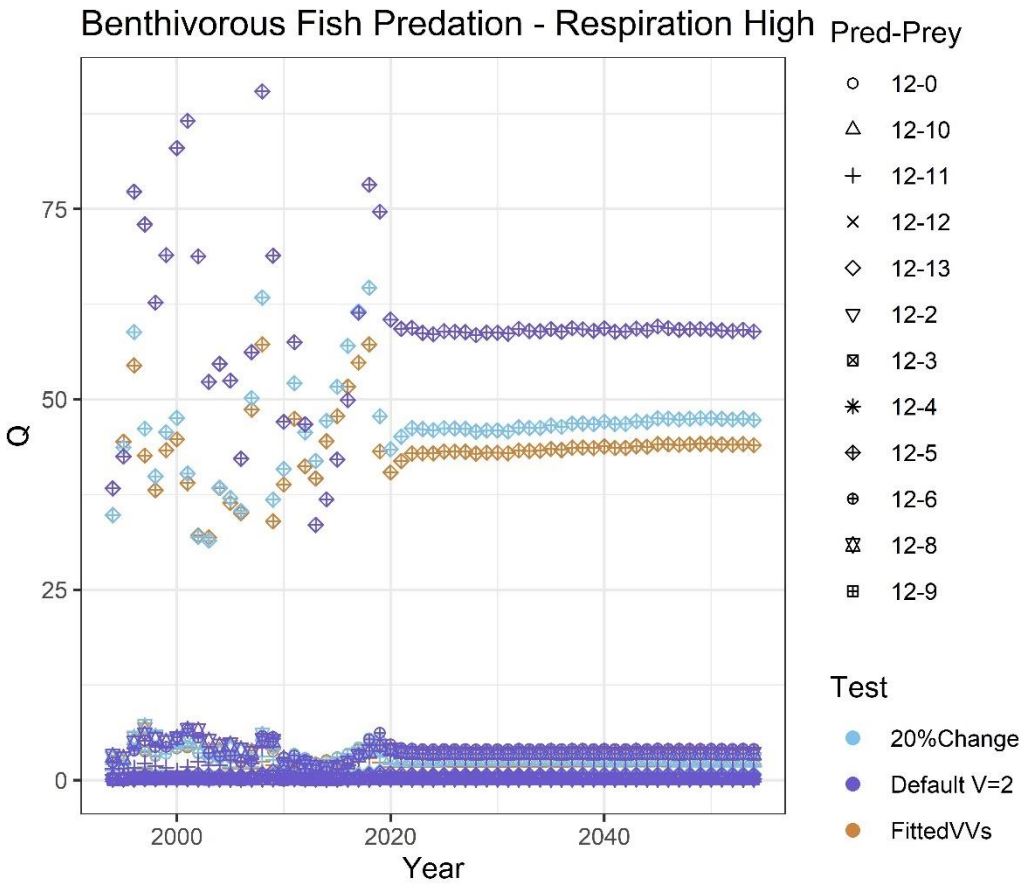


Supplemental Figure B4.4: Rpath Annual Qlink output for the high warming respiration model version testing the impact of different vulnerability values. Q represents consumption, or the energy passing between the predator and prey. The shapes denote different predator prey interactions. The legend gives predator code – prey code (Supplemental Table A1.1). Only interactions where benthivorous fish are the predator are shown. The fitted vulnerability for the strong interaction was 1.4582 for 12-5.

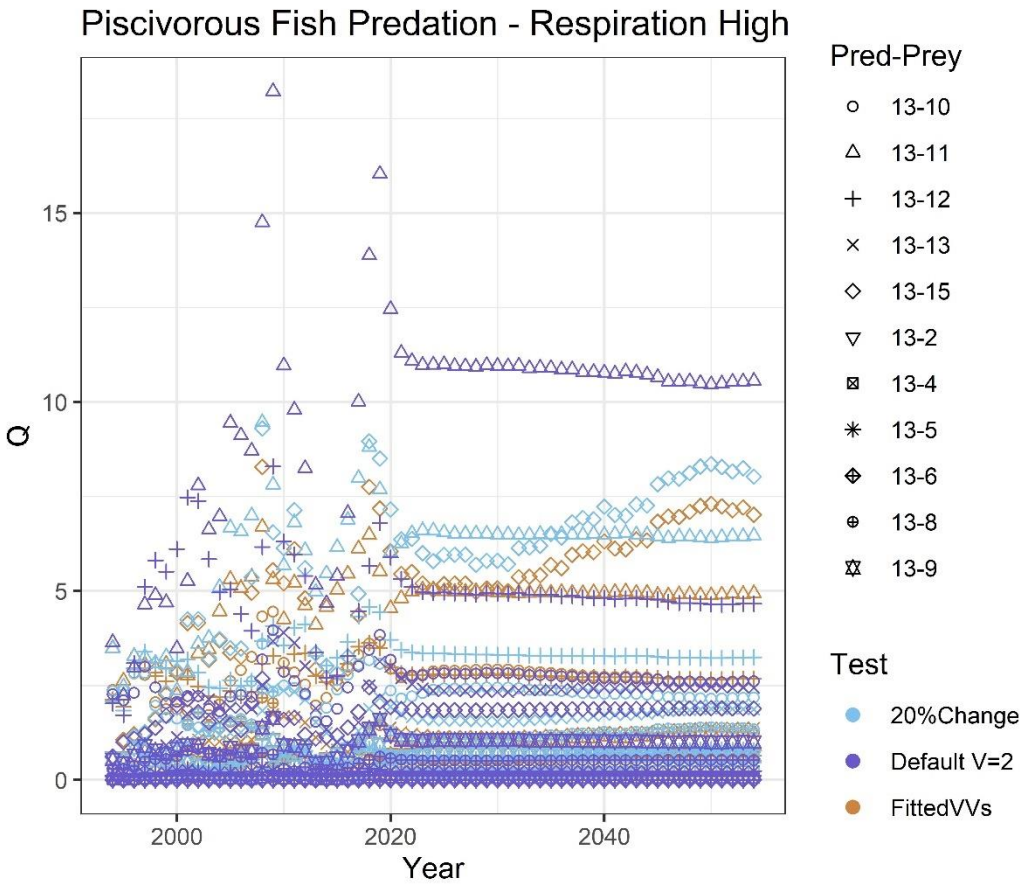


Supplemental Figure B4.5: Rpath Annual Qlink output for the high warming respiration model version testing the impact of different vulnerability values. Q represents consumption, or the energy passing between the predator and prey. The shapes denote different predator prey interactions. The legend gives predator code – prey code (Supplemental Table A1.1). Only interactions where piscivorous fish are the predator are shown. Fitted vulnerabilities for the strong interactions were 1.5325 for 13-11, 1.001 for 13-12, 1000 for 13-15, and 1.0 for 13-10.

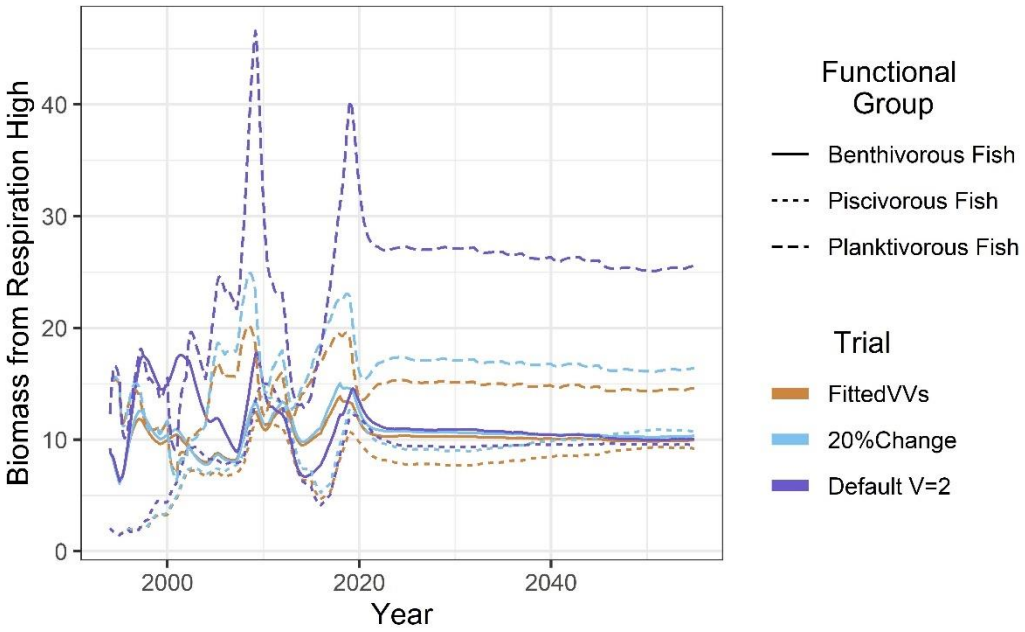


Supplemental Figure B4.6: Fish biomass output from the high warming respiration version of the model run with different vulnerability values.

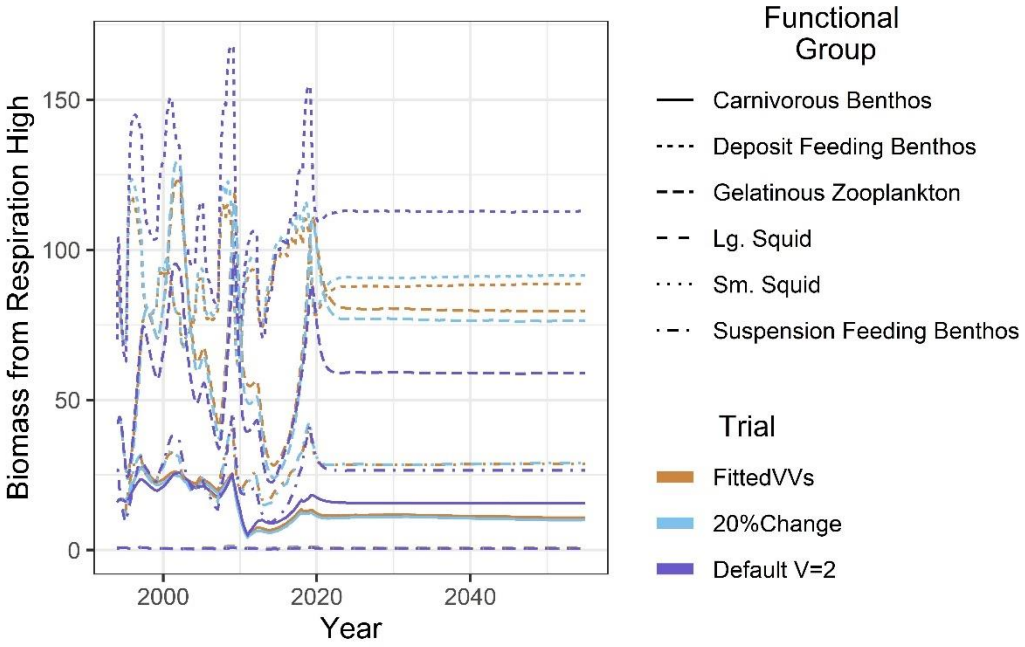


Supplemental Figure B4.7: Biomass output of select functional groups from the high warming respiration version of the model run with different vulnerability values.

Supplemental Table B4.2: Ecosystem level outputs from the 2054 projections of the different model versions. Production is the sum of catch, predation mortality, and natural mortality. The Rpath parameter representing that metric is shown in parentheses. The 'outside' group of Rpath, representing energy exiting the modeled system, was excluded from these calculations. Units are $g/m^2$.

| Parameter | Base | Cons High | Cons Low | Resp High | Resp Low |
|---|---|---|---|---|---|
| Consumption (*FoodGain*) | 11470.60 | 11478.38 | 11476.16 | 11471.66 | 11471.21 |
| Respiration (*ActiveRespLoss*) | 2231.29 | 2231.10 | 2231.03 | 2232.16 | 2232.08 |
| Predation (*FoodLoss*) | 5613.33 | 5619.15 | 5617.39 | 5613.01 | 5612.85 |
| Fisheries Harvest (*annual_Catch*) | 19.52 | 20.69 | 20.34 | 20.14 | 19.98 |
| Natural Mortality, non-predation (*MzeroLoss*) | 4371.22 | 4374.46 | 4373.41 | 4374.20 | 4373.34 |
| Ecosystem Production | 10004.07 | 10014.30 | 10011.14 | 10007.35 | 10006.17 |